Field Crops Research 337 (2026) 110287

Contents lists available at ScienceDirect

Field Crops Research

journal homepage: www.elsevier.com/locate/fcr

Modeling and explaining fertilizer effect heterogeneity on maize yield in Ghana using causal and predictive machine learning

Anselme K.K. Kouame [a,b,*], Gerard B.M. Heuvelink [a,c], Prem S. Bindraban [d]

[a] Soil Geography and Landscape Group, Wageningen University, PO Box 47, Wageningen 6700 AA, the Netherlands
[b] International Fertilizer Development Center (IFDC), Muscle Shoals, AL 35661, USA
[c] ISRIC – World Soil Information, PO Box 353, Wageningen 6700 AJ, the Netherlands
[d] Africa Rice Center, Blvd. Francois Mitterand, Abidjan 01 BP 4029, Côte d'Ivoire

ARTICLE INFO

Keywords:
Yield response
Fertilizer use efficiency
Agro-ecological zones
Precision agriculture
Causal machine learning
Data-driven modeling
Exchangeable aluminum

ABSTRACT

Context: Maize is a key staple crop in Ghana, yet yields remain low (20–40 % of potential). Although fertilizer is promoted to enhance productivity, adoption is limited by highly variable yield responses.
Objective: This study analyzed spatial and environmental drivers of fertilizer effect heterogeneity using 2854 yield observations from randomized controlled trials and 10,916 pairwise absolute yield response to fertilizer (AR) estimates.
Methods: Causal forest (CF) and boosted random forest (BRF) models to estimated fertilizer effects, with BRF performance evaluated via a 10 × 10 nested cross-validation and grid search. SHapley Additive exPlanations and Accumulated Local Effects analyses identified key drivers of fertilizer effect heterogeneity and quantified the magnitude of their influence on fertilizer yield effect.
Results and conclusions: Fertilizer effect varied widely (–4.7–8.9 t ha^{-1}), with the Sudan Savannah showing the highest median AR (2.8 t ha^{-1}) and the Forest-Savannah Transition the lowest (0.9 t ha^{-1}). BRF outperformed CF in predicting fertilizer effects (ME: –0.06–0.05 t ha^{-1} vs. –0.19 t ha^{-1}, RMSE: 1.17–1.23 t ha^{-1} vs. 1.3 t ha^{-1}, MEC: 0.32–0.38 vs. 0.24 and CCC: 0.46–0.54 vs. 0.34). Key determinants of fertilizer effect heterogeneity included both climatic variables (Palmer Drought Severity Index [PDSI], vapor pressure deficit, rainfall) and soil properties (silt content, exchangeable aluminum). PDSI emerged as the dominant driver of fertilizer effect heterogeneity in the entire data set. However, the relative importance of soil versus climate varied spatially: soil properties were the main drivers of fertilizer effect in the Semi-Deciduous Forest and the Forest-Savannah Transition, whereas climatic variables played a stronger role in northern zones. Fertilizer yield effect increased by 0.4–1.6 t ha^{-1} with increasing PDSI, indicating that improved moisture availability enhances fertilizer use efficiency. Overall, optimal moisture conditions (PDSI > –2.0), the use of hybrid seeds, and the application of briquette fertilizer all contributed to higher fertilizer effects, whereas drought conditions substantially reduced them. Furthermore, fertilizer effect decreased by 0.2–1.4 t ha^{-1} as silt increased from 9 % to 30 %, and by 0.3–0.6 t ha^{-1} as exchangeable aluminum increased from 36 to 221 mg kg^{-1}.
Significance: This study presents the first large-scale, data-driven assessment of fertilizer yield effects heterogeneity in Ghana, integrating causal and predictive machine learning with explainable AI. Findings support tailored fertilizer strategies by agro-ecological zones to reduce farmer risk and promote sustainable intensification.

1. Introduction

Maize is the most important cereal crop in Ghana, playing a critical role in the country's agriculture sector (SRID/MoFA, 2021). It is a vital food source for millions of people and contributes significantly to both the national economy and food security. The importance of maize to Ghana's agricultural sector cannot be overstated, yet local maize grain yields remain low, averaging ~ 2.4 t ha^{-1} (SRID/MoFA, 2021), significantly below the potential grain yield of 7–9 t ha^{-1} (Boullouz et al., 2022; Simperegui et al., 2023; Donkor et al., 2025). Numerous studies have identified declining soil fertility, driven largely by nutrient mining and soil erosion, as a primary cause of low maize grain yields in Ghana

* Corresponding author at: Soil Geography and Landscape Group, Wageningen University, PO Box 47, Wageningen 6700 AA, the Netherlands.
E-mail address: anselme.kouame@wur.nl (A.K.K. Kouame).

https://doi.org/10.1016/j.fcr.2025.110287
Received 19 June 2025; Received in revised form 14 November 2025; Accepted 7 December 2025
Available online 12 December 2025

(Bashagaluke et al., 2018; Essel et al., 2020). For instance, Bationo et al. (2018) estimated that soils in Ghana approximately around 35 kg nitrogen (N), 4 kg phosphorus (P), and 20 kg potassium (K) per hectare annually across all Ghana' agro-ecological zones (AEZs).

Application of fertilizers has been widely advocated as a key intervention to increase maize grain yields and has garnered substantial attention in both agricultural research and practice (Falconnier et al., 2023; Kouame et al., 2023; 2025a). Fertilizers play a pivotal role in enhancing crop productivity by replenishing soil nutrients depleted through crop uptake and erosion (Uwiragiye et al., 2022), while promoting both healthy plant growth and maintaining soil health (Dimkpa et al., 2023). Although fertilizers are widely used in Ghana, expected yield gains from fertilizer application are not consistently achieved. The effect of fertilizers on maize yield exhibits significant variability across AEZs, increasing investment risks and undermining farmers' motivation and ability to sustain fertilizer use in subsequent seasons (Nziguheba et al., 2021).

The observed low and variable fertilizer use efficiency suggests low economic returns to farmers and can lead to environmental damage, as excess nutrients not taken up by crops are often lost through leaching, runoff, or gaseous emissions, contributing to water pollution, soil degradation, and greenhouse gas emissions (Penuelas et al., 2023). Determining the causes of variability in the effect of fertilizers on yield requires analyzing the overall effectiveness of fertilizer application across the target area and how the effects vary across diverse location-specific conditions. Understanding fertilizer effect variability is essential for developing site-specific fertilizer recommendations and designing target agronomic interventions for optimizing resource allocation. Moreover, by identifying the underlying causes of this variability, one can better understand the drivers of low fertilizer use efficiency and thus identify concrete measures to enhance overall fertilizer effectiveness. However, the process of isolating the fertilizer effect and identifying the main factors influencing it, such as soil characteristics, climatic and weather conditions, microbial activity, and management practices, remains inherently complex due to their non-linear, spatial, and temporal interactions (Nziguheba et al., 2021). Agronomists have historically assessed the effect of fertilizer application on crop grain yield using randomized controlled trials randomized controlled trials (RCTs), which are widely regarded as the gold standard for causal inference due to their ability to provide robust estimates of treatment effects. In RCTs, fertilizer effectiveness is commonly quantified by estimating its average treatment effect using analysis of variance, a method that partitions the total variability in yield into components attributable to treatment and error (Fisher, 1992). However, this implicitly assumes that the fertilizer effect is uniformly applicable across all spatially distributed individual trials;. it is limited by its reliance on mean effects, which may obscure significant heterogeneity in fertilizer effects that can occur due to site-specific baseline characteristics. To address this limitation, agronomic researchers frequently analyze the grain yield absolute response to fertilizer (AR), defined as the pairwise difference between yields between yield in fertilized plots (Y_f) and yields in control plots (Y_c) randomized controlled trials, using linear regression models (Ronner et al., 2016; Sileshi et al., 2022). Although parametric regression models offer valuable insights into the influence of covariates on AR, they depend critically on the correct specification of the model; in high-dimensional settings, the assumptions of linearity and additivity often fail to capture the complex non-linear effects and interactions among fertilizer inputs, soil characteristics, climatic and weather conditions, and crop varieties. This inadequacy underscores the need for advanced statistical techniques, such as machine learning (ML) models, which are better suited to accommodate the intricate and non-linear nature of these effects and interactions (Dehghanisanij et al., 2023; 2024).

Recent studies have increasingly favored predictive ML models over traditional linear regression for estimating the effects of fertilizers rates. For instance, Coulibali et al. (2020) and Abera et al. (2022) utilized agronomic trial data alongside ML techniques, including k-nearest neighbors, random forest (RF) model, neural networks, and Gaussian processes, to estimate the effects of the rate of nitrogen fertilizer (NF), phosphorus fertilizer (PF), and potassium fertilizer (KF) on potato and wheat yields, respectively. Similarly, Tanaka et al. (2024) implemented a series of predictive ML models to develop fertilizer recommendations specifically tailored to the environmental conditions in Gifu, Japan, while Heerwaarden et al. (2023) employed RF models to assess the variability and predictability of fertilizer effects on grain legume farms in East and West Africa. In addition, Kouame et al. (2025b) applied a conditional RF model to predict the spatial and seasonal effects of sulfur fertilizer (SF) on soybean yields in Ghana.

Despite their growing adoption in agricultural research for tasks such as fertilizer recommendation development and yield response estimation, predictive ML models are fundamentally designed for correlation-based prediction rather than causal inference (Feuerriegel et al., 2024). Kakimoto et al. (2022) demonstrated that even highly accurate yield predictions with ML models do not necessarily translate into reliable estimates of NF effects on yield. Similarly, Thorburn et al. (2024) found that estimated crop yields alone are poor proxies for determining optimal NF requirements. Moreover, directly incorporating ML predictions into conventional effect estimation formulas can lead to "plug-in bias" in the measured effect (Moccia et al., 2024). When predictive ML is used to quantify the fertilizer effect and explain its variability, the approach typically involves predicting yield or AR in a manner analogous to standard regression models, without explicitly accounting for the causal structure or treatment allocation mechanism.

This lack of causal interpretability of predictive ML models has spurred the development of causal machine learning (CML) methods, which are specifically designed to infer causal relationships rather than mere correlations (Chernozhukov et al., 2016). In agricultural research, CML techniques have been applied to evaluate the effects of tillage practices (Deines et al., 2019), to assess the impact of weather on agricultural productivity (Stetter and Sauer, 2021), and to investigate the influence of digital agriculture on crop yields (Tsoumas et al., 2023). Furthermore, CML has been used to quantify the benefits of crop rotations (Kluger et al., 2022) and, in simulated wheat yield studies, to outperform traditional ML in estimating site-specific economically optimal NF rates (Kakimoto et al., 2022). In this study, we combined two complementary ML approaches to better understand how maize yield responds to fertilizer. First, we used a Boosted Random Forest (BRF) model to predict the AR. This helped us predict where fertilizer is likely to be most beneficial. We then used a causal forest (CF) (Wager and Athey, 2018), which estimates how the effect of fertilizer varies across different conditions and provides valid confidence intervals (CI) for these estimates. CF builds on the flexibility of RF, handling many variables and complex interactions without needing to predefine the structure of the model. By combining these two approaches – one focused on prediction and the other on causal inference, we aimed to address both the need for accurate, site-specific fertilizer effect predictions and a deeper understanding of where and for whom applied fertilizer is most effective.

Our study addressed four primary research questions: (i) To what extent do fertilizer effects on maize yield vary across Ghana's AEZs? (ii) How accurately can CF estimate fertilizer effects compared with a strong predictive benchmark such as BRF? (iii) How do local climate conditions, soil properties, and management practices shape fertilizer responsiveness, and which factors exert the strongest influence? and (iv) Can these insights be translated into site-specific fertilizer recommendations that improve resource efficiency? Leveraging 2854 maize yield observations from randomized fertilizer trials across Ghana, combined with detailed environmental and management covariates, we integrated CML with explainable artificial intelligence techniques to quantify and interpret heterogeneity in fertilizer yield responses. Our approach moves beyond average treatment effects to provide spatially and context-specific insights, supporting both the reduction of fertilizer

losses in low-responsive areas and the targeting of investment to high-potential regions to improve productivity and sustainability.

2. Materials and methods

2.1. Study locations, climate, and period

Maize fertilizer trials were conducted across four AEZs in Ghana, Sudan Savanna (SS), Guinea Savannah (GS), Forest-Savanna Transition (FST), and Semi-Deciduous Forest (SDF) (Fig. 1**a**). These zones together form the country's main maize-producing region and represent its agricultural breadbasket (Tetteh et al., 2018). The dataset spans a 17-year observational period (Fig. 1**b**). Planting schedules were synchronized with the AEZs' rainfall regimes: the SS and GS zones experienced unimodal rainfall patterns, while the FST and SDF exhibited bimodal seasonal distributions (Röhrig et al., 2019). Across AEZs, mean growing season temperatures ranged from 22.7 ± 0.2°C to 31.2 ± 0.9°C, with cumulative rainfall (RAIN) varying between 542 ± 109.3 mm and 741.4 ± 146.1 mm (Table 1, Table S1). Elevation gradients differed markedly by AEZ: 218–445 m in the SDF, 129–322 m in the FST, 122–342 m in the GS, and 165–360 m in the SS (Table S2). Soil properties exhibited pronounced inter-AEZ variability (Table S1). Soils in all AEZs featured a sandy texture (SAND; 66.6 ± 5.9 %), and low soil organic carbon (SOC; 1.4 ± 0.8 g kg^{-1}) (Table 1, Table S1). Soils in the SS and GS zones had a shallow profile (69.8 ± 25.1 cm root zone depth), contributing to inherently lower fertility relative to the SDF and FST zones, where soils were deeper (113.2 ± 15.9 cm) and more chemically fertile (Tables S1 and S2).

2.2. Data collection

Maize grain yields (t ha^{-1}) were sourced from two primary datasets: (i) on-station trial data (n = 1622) reported in Bua et al. (2020), and (ii) on-station trial data (n = 3346) from experiments conducted by the International Fertilizer Development Center (IFDC). Detailed methodologies for data collection are provided in Methods S1 and Bua et al. (2020). Geographic coordinates were recorded for each experimental site, all of which were rainfed and involved maize grown in monoculture. To qualify for inclusion, experiments were required to be field-based and include at least one paired dataset (i.e., a control plot without fertilizer and a treatment plot with fertilizer) under near-identical microclimatic, soil, and vegetation conditions. In addition, experiments were required to have been conducted in terrestrial ecosystems with documented application rates for various fertilizers (NF, PF, and KF), span at least one full growing season, and involve multiple fields with consistent fertilizer treatments and corresponding control plots. For experiments with multiple control and treatment plots, the AR was estimated for each unique pairing of control and fertilizer-treated plots, resulting in 23,040 AR data points derived from 4968 yield observations.

For the AR analysis, paired control and treatment plots were required. However, the available dataset exhibited substantial variability in NF, PF, and KF application rates, with NF having the widest variability, ranging from 12 kg ha^{-1} to 250 kg ha^{-1} and both PF and KF ranging from 8 kg ha^{-1} to 90 kg ha^{-1} (Fig. S1 and S2). An ideal experimental design would entail a binary treatment structure, comparing control plots with uniformly fertilized plots receiving fixed rates of NF, PF, and KF. A stringent approach would involve restricting the analysis to yield data from experiments where identical fertilizer rates were

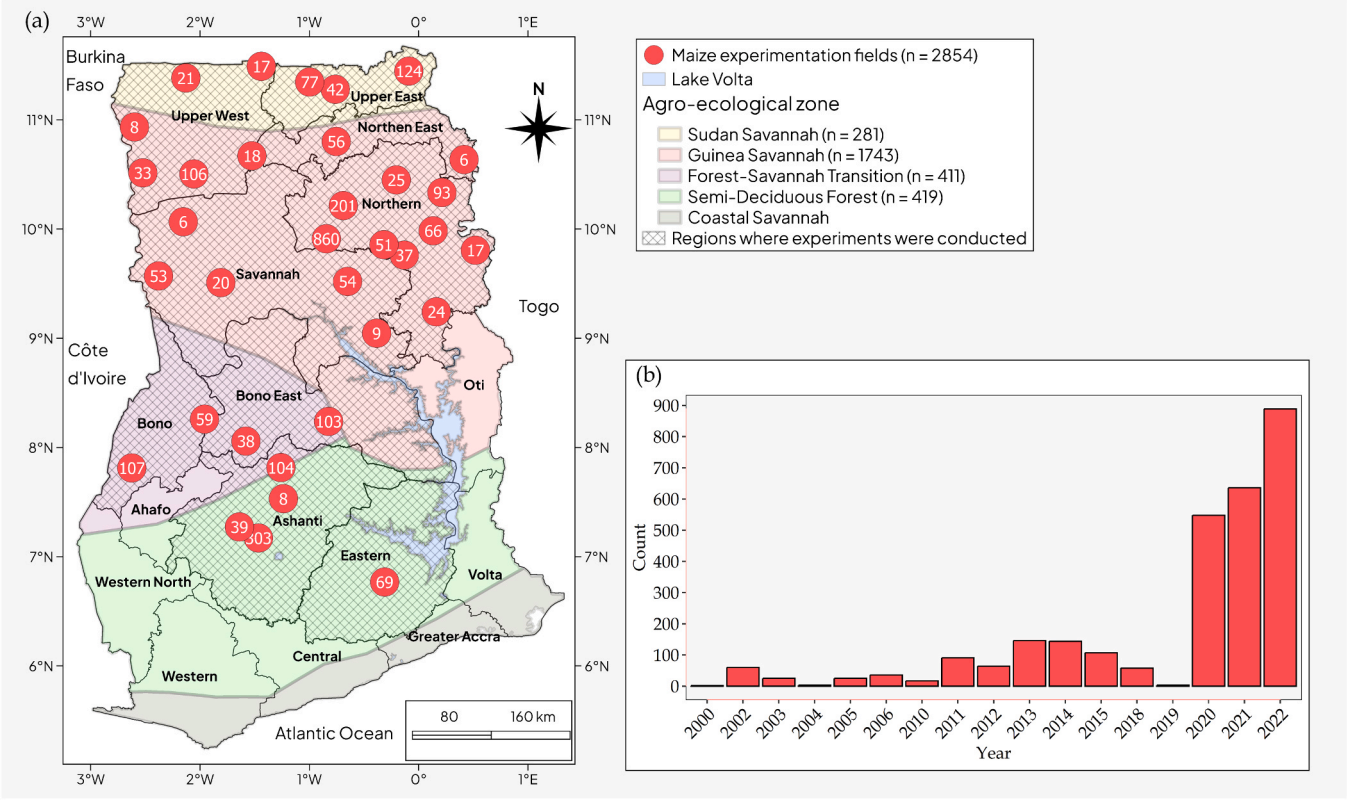

Fig. 1. (a) Spatial distribution of experimental maize fields (n = 2854) across Ghana's agro-ecological zones (AEZs). Field locations are aggregated into uniform 16 km radius clusters (red circles), with numerical labels indicating the count of field sites per cluster. Background shading represents distinct AEZs, demonstrating national-scale coverage of the experimental network. Many field locations are in close proximity, and the AEZ map was adapted from Yamba et al. (2023). Notably, 61 % of the experimental data come from the Guinea Savannah zone. **(b)** Histogram showing the temporal distribution of maize experimentation data in Ghana. The majority (71 %) of the data were collected in 2020, 2021, and 2022.

Table 1
Summary of continuous covariate (gridded climate, soil, and terrain) data used in the boosted random forest and causal forest model.

Continuous covariates†	Acronym	Unit	Min	Max	Mean ± SD	Median	Source
Climate							
Cumulative rainfall	RAIN	mm	285.4	1031.4	684.5 ± 160	660.4	
Maximum temperature	TMAX	°C	28.9	34.3	30.7 ± 0.9	30.6	
Minimum temperature	TMIN	°C	21.9	24.7	23 ± 0.5	23	ERA5
Cumulative solar radiation	SRAD	kWh m^{-2}	645.8	1091.8	836.5 ± 56.3	847.9	
Mean wind speed	MWS	m s^{-1}	1	2.1	1.7 ± 0.2	1.8	
Vapor pressure deficit	VPD	kPa	0.6	1.5	0.9 ± 0.2	0.9	TerraClimate
Palmer Drought Severity Index	PDSI	-	-6.3	1.9	-3 ± 2	-3.2	
Soil chemical property							
pH	pH	-	5.3	6.4	6 ± 0.2	6	
Exchangeable phosphorus	P	mg kg^{-1}	5	12.5	7.3 ± 1	7.2	
Exchangeable sulfur	S	mg kg^{-1}	4	8	4.8 ± 0.8	4.5	
Total N	N	g kg^{-1}	0	0.3	0.1 ± 0	0.1	
Organic carbon	SOC	g kg^{-1}	0.7	3.9	1.4 ± 0.8	1.2	
Exchangeable calcium	Ca	mEq 100 g^{-1}	1.6	5.5	2.8 ± 0.7	2.7	
Exchangeable magnesium	Mg	mEq 100 g^{-1}	0.5	2.4	1 ± 0.2	0.9	iSDAsoil
Exchangeable potassium	K	mEq 100 g^{-1}	0.1	0.3	0.2 ± 0	0.2	
Effective cation exchange capacity	ECEC	cmol (+) kg^{-1}	5	12.5	7.3 ± 1.3	7.2	
Exchangeable iron	Fe	mg kg^{-1}	53.6	98.5	68.9 ± 5.6	65.7	
Exchangeable aluminum	Al	mg kg^{-1}	36.6	221.4	121.1 ± 30.8	109.9	
Exchangeable zinc	Zn	mg kg^{-1}	0.5	3.5	1 ± 0.8	0.6	
Base saturation	BS	%	29.8	84.3	53.7 ± 12.1	53.7	
Soil physical property							
Clay	CLAY	%	6	25	13.9 ± 3.5	13	
Sand	SAND	%	49	83	66.6 ± 5.9	68	iSDAsoil
Silt	SILT	%	9	31	19.5 ± 3.7	19	
Long term mean soil moisture	SMgp	mm	26.7	249.2	132.3 ± 45.2	134.2	TerraClimate
Root zone depth	RD	cm	24	150	84.8 ± 30.4	82	
Soil moisture content at saturation	SMS	%v (volumetric)	33	48	40.2 ± 3.2	39	SoilGrids
Soil moisture content at wilting point	SMWP	%v (volumetric)	12	22	15.5 ± 2.1	15	
Water holding capacity	WHC	mm	23	135	64.7 ± 23.9	62	
Terrain							
Elevation	ELV	m	116	445	211.7 ± 63.8	182	
Topography wetness index	TWI	-	5.7	11.7	9.4 ± 1.1	9.6	SRTM Plus V3
Stream power index	SPI	-	0	12.8	1.1 ± 1.5	0.7	
Slope	SLP	°	0.1	2.7	0.5 ± 0.4	0.4	

† the description of each continuous variable is reported in the supplementary Table S3
SD: standard deviations

applied. However, such an approach would drastically reduce the sample size, thereby compromizing the robustness of subsequent ML-based statistical analyses and inferences. To mitigate the loss of data but also avoid having treatment plots with insufficient fertilizer application rates, a filtering criterion was applied: only treatment plots meeting or exceeding NF $\geq$ 45 kg ha^{-1}, PF $\geq$ 30 kg ha^{-1}, and KF $\geq$ 30 kg ha^{-1} – along with their corresponding control plots – were retained for further analysis. These thresholds were informed by maize fertilization recommendations for Ghana, as established in Tetteh et al. (2017). Following this selection process, the final dataset comprised 2854 yield observations (Fig. 1**a**) and 10,916 AR observations, with treatments dichotomized into control (T = 0, n = 501) and fertilized (T = 1, n = 2353).

2.3. Covariate sources

In this study, we incorporated a range of covariates – including topographical, meteorological, and soil properties; mode of fertilizer application; and maize variety (Tables 1 and 2) – to quantify and elucidate the variability in fertilizer effects. Experimental site elevation (ELV) was obtained from the NASA Digital Elevation Model (~30 m resolution) (Farr et al., 2007). From ELV we derived the slope (SLP), topographic wetness index (TWI), and stream power index (SPI) using the terra package (version 1.8–42) (Hijmans et al., 2022) in R (version 4.4.3) (R Core Team, 2025) with a 3 × 3 window size. TWI is a proxy of the spatial distribution of moisture integrating slope and terrain attributes that affect the soil-water balance and erosion, whereas SPI quantifies the erosive power of flowing water and its implications for soil quality and agricultural viability. Low SPI values denote reduced erosion potential, while high SPI values indicate an important risk of soil erosion. High TWI values are typically associated with deeper, wetter soils that are prone to saturation and water accumulation, in contrast to lower TWI values that are indicative of steeper, drier areas.

To account for interannual variability in weather, we computed cumulative precipitation (RAIN), cumulative solar radiation (SRAD), minimum (TMIN) and maximum (TMAX) temperatures, mean wind speed (MWS), vapor pressure deficit (VPD), long-term mean soil moisture (SMgp), and the Palmer drought severity index (PDSI) (Palmer, 1965) during the maize growing season, which differed from AEZ to AEZ. Weather data were sourced from ERA5 at ~11 km resolution (Hersbach et al., 2020) and TerraClimate at ~4 km resolution (Abatzoglou et al., 2018). Additionally, for each plot-level observation, soil chemical and physical properties were extracted from the Innovative Solutions for Decision Agriculture (iSDA) map at 30 m resolution for the 0–20 cm topsoil layer, while root zone depth (RD), root zone water-holding capacity (WHC), soil drainage status (DRAIN), soil moisture content at wilting point (SMWP), and soil moisture content at saturation (SMS) were retrieved from SoilGrids at ~250 m resolution (Poggio et al., 2021; Turek et al., 2023).

The maize cultivars evaluated in this study comprised 15 distinct varieties, stratified into two categories: open-pollinated varieties (OPVs), which constituted 93 % of the dataset, and hybrid varieties, representing 7 % (Table 2). Fertilizers were administered through two distinct application modalities: 25 % as subsurface briquettes placed in planting holes and 75 % as broadcast granular applications on the soil surface. Experimental sites were predominantly imperfectly drained (57 %), with the remainder classified as well-drained (43 %). Categorical variables – including cultivar type (VAR), fertilizer placement

Table 2
Categorical covariates with their category level used in the boosted random forest and causal forest models.

Categorical variables	Acronym	Description and rationality	Levels	Source
Management				
Variety	VAR	Maize varieties differ in their genetic makeup, growth characteristics, yield potential, and resilience to environmental stresses (e.g., drought, pests, and diseases). So, different varieties can respond differently to fertilizers and environmental conditions, which can significantly influence impact yield outcomes.	Hybrid OPV	Bua et al. (2020); IFDC
Fertilizer placement	FPLACE	Fertilizer can be applied in various ways, including broadcasting, banding, side-dressing, or foliarly. The mode of application affects how nutrients are distributed and absorbed by plants. The efficiency of nutrient uptake can vary with the method of application, influencing maize growth and yield. For instance, banding fertilizer near the root zone can improve nutrient availability and reduce losses compared to broadcasting	Hole Soil surface	Bua et al. (2020); IFDC
Soil physical property				
Drainage status	DRAIN	Drainage refers to the soil's ability to remove excess water, which prevents waterlogging. Good drainage is essential for root health and nutrient absorption, especially in regions with heavy rainfall. Poor drainage can lead to waterlogging, reducing root oxygen availability and nutrient uptake, ultimately affecting yield.	Imperfect Well	SoilGrids

method (FPLACE), and soil drainage status (DRAIN) – were transformed into multiple binary variables via one-hot encoding using the "dummyVars()" function in the caret R package (version 7.0–1) (Kuhn, 2008).

2.4. Machine learning inference

The primary objective of this study was to estimate the effect of fertilizer application on maize grain yield, analyze the variability of this effect, and identify the factors influencing it. To achieve this, we employed three distinct approaches, using BRF and CF.

2.4.1. Approach 1 – traditional absolute yield response

A BRF is an ensemble learning method that combines the strengths of RF and boosting to improve prediction accuracy (Ghosal and Hooker, 2020). It builds a sequence of regression forests, where each forest is trained to correct the residual errors of the previous one, thereby reducing bias iteratively. BRF was implemented as a stagewise additive model using gradient boosting with forests as base learners though the grf R package (version 2.5.0) (Tibshirani et al., 2024). We first calculated the AR for each paired control-treatment observation, defined as the difference in yield between fertilized and control plots, which could be done because the data are from randomized controlled trials. We then constructed a predictive BRF model that predicts AR ($\widehat{AR}_{BRFy}$) using the covariates (X, the pre-treatment characteristics) in Tables 1 and 2, excluding the binary fertilizer treatment indicator T (where $T \in \{0, 1\}$). The model predicts AR, thereby capturing fertilizer effect variability attributable solely to factors other than the fertilizer treatment.

2.4.2. Approach 2 – predictive BRF fertilizer effect estimation

In this approach, a BRF model was developed to predict maize grain yield (Y) using all yield data (control as well as treatment) and the full set of covariates X, including the binary fertilizer treatment variable T. The fertilizer effect was next quantified using Eq. (1), which computes the difference between the predicted yield with fertilization ($\widehat{Y}_i(1)$) and without ($\widehat{Y}_i(0)$), conditional on the observed covariates $X_i = x_i$:

$$\widehat{AR}_{BRF\Delta y,i} = (\widehat{Y}_i(1) - \widehat{Y}_i(0)) \mid X_i = x_i,\ i = 1,\ldots,n \quad (1)$$

where, n denotes the number of observations. This formulation is analogous to the individual treatment effect in causal inference but adapted to quantify fertilizer-induced yield gains.

This method leverages the BRF model's ability to model non-linear interactions and heterogeneity, providing an estimate of the fertilizer effect that also accounts for the influence of other covariates. To fine-tune the BRF models in Approach 1 and Approach 2, a nested 10 × 10 cross-validation was employed, which included an inner loop for hyperparameter optimization and an outer loop for evaluating generalization performance (Krstajic et al., 2014). First, the pooled dataset was randomly split into 10 equal parts using the "createFolds()" function of the caret R package (version 7.0–1) (Kuhn, 2008), which constituted the outer loop of ten folds. Each fold of the outer loop was used once as a test set, while the remaining nine served as the training set. Within each of these training sets, an inner loop performed its own cross-validation – in our case, also 10-fold – to optimize a model's hyperparameters. This dual-layer structure ensured that the test sets from the outer loop were never used for model calibration or hyperparameter tuning. This prevents data leakage, minimizes overfitting, and provides an unbiased assessment of a model's predictive capabilities (Rosenblatt et al., 2024). Mean Squared Error (MSE) was considered as the loss function in the BRF models training. For each BRF model, we performed a grid search to optimize the hyperparameters of interest: the number of covariates to consider at each split (mtry, tested at values of 15, 26, and 34), and the minimum number of observations allowed in each terminal node (min.node.size, tested at values of 5, 10, 15, and 20). The number of trees was set to 5000.

2.4.3. Approach 3 - causal forest fertilizer effect estimation

To explicitly estimate the causal effect of fertilizer on maize yield, we applied the CF model. Although CF shares structural similarities with RF, both being tree-based methods, their objectives differ fundamentally. RF is designed to build a predictive model by partitioning the data into subsets where yield variability is minimized, thus enhancing prediction accuracy. In contrast, CF specifically targets causal inference by dividing the data into subsets based on similar covariate profiles, where differences in fertilizer response are maximized. Detailed descriptions of CF are provided in (Wager and Athey, 2018). The CF method addresses the fundamental challenge of causal inference – the fact that we cannot simultaneously observe both the treated and untreated yield for the same plot (Holland, 1986). According to the Splawa-Neyman (1923) and Rubin (1974) potential outcomes' framework, also called the Rubin Causal Model (Imbens and Rubin, 2015), we denote $Y_i^{(1)}$ as the counterfactual potential yield with fertilizer and $Y_i^{(0)}$ as the counterfactual potential yield without it for plot i. The CF model estimates the conditional average fertilizer effect for a given set of covariates x_i as:

$$\widehat{AR}_{CF,i} = \mathbb{E}\left[Y_i^{(1)} - Y_i^{(0)} \mid X_i = x_i\right],\ i = 1,\ldots,n \quad (2)$$

where, $\mathbb{E}$ represents mathematical expectation and n denotes the number of observations.

For the prediction of $\widehat{AR}_{CF}$, CF relies on several key assumptions (Wager and Athey, 2018). First, it assumes unconfoundedness – that is, it assumes that after conditioning on covariates, the assignment of fertilizer is effectively random. Second, it requires an overlap assumption, which ensures that each field has a positive probability of both receiving the fertilizer treatment and serving as control plot, meaning that the

so-called propensity scores for all plots are higher than zero and lower than one. Third, the Stable Unit Treatment Value Assumption is assumed, which stipulates that the potential outcomes of any field are not influenced by the treatment assignments of other units (Wager and Athey, 2018). In our study, all three assumptions are met because the data are from randomized controlled trials.

For CF implementation, we used the grf R package (version 2.4.0) (Tibshirani et al., 2024). The analysis started with fitting two RF models to estimate the conditional expected maize grain yield and propensity score based on the available covariates. These estimates were then input into the grf "causal_forest()" function to estimate $\widehat{AR}_{CF}$. To account for the imbalance in the treatment allocation, where the number of fertilized plots (treated units) exceeded the non-fertilized plots (control units), sample weights were applied to ensure balanced representation during CF model fertilizer effect estimation. Specifically, each treated unit (T = 1) was assigned a weight of 1, while control units (T = 0) were weighted by the ratio of treated to control observations. This upweighting of control observations helped mitigate potential bias arising from unequal group sizes, ensuring that the CF estimator accounted for disparity in the dataset. CF implementation in this paper adheres to the CF methodology outlined in Athey and Wager (2019).

The CF model was built over 5000 causal trees ("num.trees") and used the "tune.parameters" option in the grf package to allow automatic tuning of the "mtry" hyperparameters using cross-validation (Table S4). However, we set the hyperparameter "alpha" to 0.001 instead of keeping the default value of 0.05, as recommended in Jakobsen (2023) when some of the categorical covariates are very unbalanced. CF inherently employs cross-fitting to ensure robust and unbiased treatment effect estimates (Chernozhukov et al., 2016). Cross-fitting ensures that the data used to create splits are distinct from the data used to estimate $\widehat{AR}_{CF}$. By default, the grf package applies twofold cross-fitting when the "honesty" option is set to "TRUE". In this study, we complemented this by employing a leave-one-out cross-fitting procedure to predict $\widehat{AR}_{CF}$, as recommended in Athey et al. (2018), to further enhance the robustness of the results.

Notably, the FPLACE covariate was not used in CF. In causal inference frameworks such as CF, covariates must represent pre-treatment characteristics applicable to both treated (T = 1) and untreated (T = 0) units. Since FPLACE is only observed in treated plots and imputed as 0 for controls, it violates the pre-treatment assumption required by CF. To ensure comparability among covariates and improve model performance, all numerical covariates in Table 1 were standardized using centering and scaling. Centering involved subtracting the mean of each covariate from its individual values, resulting in covariates with a mean of zero. Scaling then divided each centered variable by its standard deviation, yielding variables with unit variance. To improve model generalizability across AEZs and years with limited representation (Fig. 1), we applied a weighted sampling during BRF and CF model fitting (Kamangir et al., 2024). This approach increases the probability that observations from under-sampled AEZ-year strata contribute to model training. Specifically, we assigned observation-level weights inversely proportional to the joint frequency of their AEZ-yield and year-yield groupings, thereby giving greater influence on rare yet equally relevant production conditions.

To evaluate the performance of the BRF models in predicting AR, we employed several metrics: (i) the root mean squared error (RMSE, in t ha^{-1}); (ii) the mean error (ME), which is the average difference between predicted and observed values (with positive values indicating systematic over-prediction and negative values indicating under-prediction); (iii) the model efficiency coefficient (MEC), an analog of the coefficient of determination as described in Nash and Sutcliffe (1970); and (iv) the concordance correlation coefficient (CCC), a normalized metric that integrates the Pearson correlation coefficient [r, (precision)] with an index of accuracy (Lin, 1989) (Methods S2). Model performance metrics (ME, RMSE, MEC, and CCC) were averaged across the outer folds of the 10 × 10 nested cross-validation. To compare fertilizer-effect predictions across the three modelling approaches, we used the r, mean absolute difference (MAD; t ha^{-1}), and mean deviation (MD; t ha^{-1}) (Methods S3). The formulas for all performance metrics are provided in Table S5, and the results are visualized using scatter density plots.

2.5. Covariate importance, main effects, and interaction influence

The relative magnitude and directional contributions (positive or negative) of covariates to the predictions of AR via BFR in Approach 1 ($\widehat{AR}_{BRFy}$), fertilizer effect estimates from BRF in Approach 2 ($\widehat{AR}_{BRF\Delta y}$), and CF fertilizer effect ($\widehat{AR}_{CF}$) in Approach 3, were quantified using SHapley Additive exPlanations (SHAP) values (Lundberg and Su-In, 2017). The SHAP value quantifies the marginal contribution of a covariate to the difference between a model's prediction for a specific instance and the baseline prediction (typically the dataset-wide mean). Rooted in coalitional game theory (Shapley, 1953), SHAP values conceptualize covariates as "players" collaborating to achieve a collective "payoff," defined as the deviation of a unit-specific prediction from the global mean prediction. In this framework, each covariate's contribution is proportionally allocated based on its marginal influence on model outcomes (Lundberg and Su-In, 2017). Mathematically, SHAP values satisfy the properties of "efficiency", "symmetry", "dummy", and "additivity", ensuring a consistent and theoretically grounded attribution of predictive variance across covariates (Young, 1985). Computational implementation of SHAP values was performed using the fastshap R package (version 0.1.1) (Brandon, 2022), with global (aggregate) and local (instance-specific) contributions to the $\widehat{AR}_{BRFy}$, $\widehat{AR}_{BRF\Delta y}$, and $\widehat{AR}_{CF}$ visualized via the "plot_shap_bar()" function in the nestedcv R package (version 7.12) (Lewis et al., 2023). Covariates identified as having the highest SHAP-based importance were further analyzed to quantify and illustrate their influence on fertilizer effect heterogeneity. Main effect magnitudes were quantified and visualized using SHAP dependence plots (SHAPDP) (Lundberg and Su-In, 2017), and accumulated local effects (ALE) plots (Apley and Zhu, 2020). SHAPDPs depict the relationship between covariate values and their corresponding SHAP values, while ALE plots estimate cumulative marginal effects by averaging prediction changes across covariate intervals (Molnar, 2025).

To assess how interactions between covariates influence fertilizer effects, two-way interactions were analyzed and visualized using two-dimensional 2D ALE plots (Apley and Zhu, 2020). Unlike partial dependence plots (PDPs) (Friedman, 2001), ALE plots account for correlations among covariates, making them more reliable when covariates are interdependent. Therefore, 2D ALE plots were preferred over 2D PDPs (Friedman, 2001) for visualizing the interaction effects of covariates on fertilizer yield effect. The 2D ALE computations followed the methodology described in Apley and Zhu (2020). The 2D ALE plot visualizations were generated using the "FeatureEffect$new()" function from the iml R package (version 0.11.3) (Molnar et al., 2018).

3. Results and discussion

3.1. Variability in observed absolute maize yield response to fertilizer

The AR in the pooled dataset (n = 10,916) ranged from –4.7 t ha^{-1} to 8.9 t ha^{-1}, with a median of 1.3 t ha^{-1} and a mean of 1.4 t ha^{-1}, indicating considerable variability (coefficient of variation [CV] = 106.7 %; Table 3). In the FST and SDF zones, AR exhibited a narrower range (–3.1 t ha^{-1} to 5.6 t ha^{-1}) and lower central tendency values (mean = 0.9 t ha^{-1}; median = 1.2 t ha^{-1}). These results underscore the geographically heterogeneous effects of fertilizer on maize grain yield. The CV of AR was highest in the FST (146.7 %) and lowest in the SDF (82.4 %). In the GS, AR values were identical to those in the pooled dataset, as 63 % of the fertilizer trial plots were in this AEZ. While most AEZs exhibited mean ARs between 1.0 t $ha^{-1}$and 1.3 t ha^{-1}, the SS stood

out with a higher mean AR (2.9 t ha^{-1}) and the lowest variability (CV = 59.2 %).

3.2. Fertilizer effect prediction

Model tuning showed that the optimal "mtry" was 26 for BRF in Approach 1, 15 for BRF in Approach 2, and 26 for CF in Approach 3. The minimum node size was 5 for BRF in Approach 1 and CF in Approach 3, and 15 for BRF in Approach 2. The "sample.fraction" and "honesty. fraction" parameters were maintained at their default value of 0.5 across all models.

Based on performance metrics, the BRF models outperformed the CF model in predicting fertilizer-induced changes in maize yield (Fig. 2**a, b, c**). In Approach 3, the CF model explained 24 % of the variability in fertilizer yield effects (MEC = 0.24), whereas the BRF models accounted for 32 % and 38 % in Approaches 1 and 2, respectively (MEC = 0.32 and 0.38). The CF model also exhibited higher bias (ME = –0.19 t ha^{-1}) and greater prediction error (RMSE = 1.30 t ha^{-1}) than the BRF models in Approach 1 (ME = –0.06 t ha^{-1}, RMSE = 1.17 t ha^{-1}) and Approach 2 (ME = 0.05 t ha^{-1}, RMSE = 1.23 t ha^{-1}). Similarly, the CCC was also lower for CF (0.34) compared with 0.46 and 0.54 for BRF in Approaches 2 and 1, respectively. Despite these performance differences, the fertilizer-effect predictions were highly consistent across the three approaches. Pearson correlation coefficients (r) between predicted fertilizer effects ranged from 0.79 to 0.87, with MAD of 0.33–0.41 t ha^{-1} and MD of 0.11–0.23 t ha^{-1} (Fig. 2**d, e, f**).

In Approach 3, the CF model estimated an average fertilizer effect on the treated plots of 1.9 t ha^{-1} (95 % CI: 1.6–2.1 t ha^{-1}), whereas the BRF model predicted mean fertilizer effects of 1.5 t ha^{-1} (Approach 1) and 1.3 t ha^{-1} (Approach 2). Notably, the CF model predicted a narrower range of fertilizer effects compared to both the observed AR and the BRF model's fertilizer effect predictions (Fig. S3). The CF model produced a narrower range of fertilizer effects than both the observed AR and the BRF predictions. It also suggested that 100 % of fertilized plots exhibited positive yield responses, compared with 99.1 % in Approach 1 and 99.7 % in Approach 2 (Fig. S3).

The observed superiority of prediction performance metrics (i.e., CCC, MEC, ME, and RMSE) of BRF over CF in predicting fertilizer effect aligns with methodological expectations but contradicts findings in Kakimoto et al. (2022). Our findings are consistent with recent work by Venkatasubramaniam et al. (2023), who found that the LASSO regression model outperformed CF in estimating treatment effect heterogeneity. The divergence in BRF and CF external validation performance (i.e., versus AR_{Obs}) arises from fundamental differences in the models objectives: BRF is algorithmically optimized to minimize prediction MSE across the entire AR_{Obs} distribution, whereas CF prioritizes unbiased estimation of conditional average treatment effects by explicitly modeling causal relationships, often at the expense of predictive precision.

The elevated fertilizer effects from AR_{Obs} calculations and $\widehat{AR}_{BRFy}$, relative to $\widehat{AR}_{BRF\Delta y}$ and $\widehat{AR}_{CF}$, likely result from the binarization of the continuous treatment variable. This simplification reduced the CF and BRF models' ability to accurately capture the dose – response relationship between fertilizer rates and maize yield. Consequently, both the CF (Approach 3) and BRF (Approach 2) may have produced attenuated fertilizer effect estimates when relying on this binary treatment representation. Additionally, the higher $\widehat{AR}_{BRF\Delta y}$ values compared to the $\widehat{AR}_{CF}$ values may be attributed to the lack of targeted regularization in BRF. In contrast, CF applies covariate adjustment and shrinkage techniques that reduce bias and tend to produce more conservative treatment effect estimates (Caron et al., 2022).

Table 3
Descriptive statistics for absolute response to fertilizer (t ha^{-1}).

	n	Min	Max	Mean±SD	Median	CV†
Pooled data	10,916	–4.7	8.9	1.4 ± 1.5	1.3	106.7
FST	2141	–3.1	5.6	0.9 ± 1.3	0.9	146.7
GS	6438	–4.7	8.9	1.3 ± 1.4	1.3	105.6
SDF	1315	–2.3	5.0	1.2 ± 1.0	1.2	82.4
SS	1022	–2.2	7.6	2.9 ± 1.7	2.8	59.2

† Coefficient of variation

3.3. Key factors influencing fertilizer effect

Globally, PDSI emerged as the most influential covariate of fertilizer effects on maize grain yield in Approaches 1 and 3, whereas soil exchangeable aluminum (Al) had the greatest contribution in Approach 2, as indicated by mean SHAP values (Fig. 3**a, b, c**). PDSI and Al exhibited contrasting contributions to fertilizer-induced yield responses, with PDSI associated with positive average contributions and Al with negative ones (Figs. 3 and S4). On average, PDSI explained 14 %, 9 %, and 17 % of the variability in fertilizer yield effects under Approaches 1, 2, and 3, respectively. In contrast, Al accounted for 5 %, 10 %, and 7 % of the variability across the same approaches (Table S6). Beyond PDSI and Al, four additional covariates – soil silt content (SILT), RAIN, WHC, and ELV – out of the top ten-ranked covariates from variable importance were shared between BRF and CF models across all three approaches. Several covariates demonstrated model-specific directions of contribution to fertilizer effect variability. For example, in Approaches 1 and 2, exchangeable calcium (Ca), magnesium (Mg), sulfur (S), total nitrogen (N), DRAIN, and TWI were associated with positive average contributions to fertilizer yield responses. In contrast, under Approach 1, these same variables showed negative average contributions to fertilizer effects. Although not among the top ten most influential covariates, two agronomic practices consistently showed positive contributions to fertilizer effects: (1) the use of hybrid maize varieties (VAR) and (2) the localized placement of fertilizer briquettes (FPLACE) directly into planting holes (Fig. 3**a, b, c**). These findings suggest that strategic cultivar selection and precision nutrient placement can enhance fertilizer performance, even if their overall explanatory power remains modest relative to dominant soil and climatic variables.

Fig. 4 presents SHAP summary plots for the BRF and CF models across the four AEZs, illustrating the influence of the top ten covariates on the effect of fertilizer on maize yield. In the SS zone, three covariates – PDSI, RAIN, and SMS – were shared among the top ten variables in both the CF and BRF models, albeit with differing rankings. PDSI and RAIN showed positive contributions to the fertilizer-induced yield response, whereas higher SMS values were associated with low fertilizer effectiveness. In the GS zone, six covariates – PDSI, VPD, Al, ELV, SILT, and RAIN – were consistently ranked among the top ten, though their relative importance varied. Notably, increases in PDSI, VPD, ELV, and RAIN were associated with enhanced fertilizer response, while higher SILT and Al levels corresponded to diminished fertilizer effectiveness. In the FST zone, three covariates – WHC, VPD, and ELV – were consistently identified among the top ten across models. An increase in WHC was associated with a reduction in fertilizer effectiveness, whereas higher values of VPD and ELV were linked to improved yield responses to fertilizer. In the SDF zone, three covariates – SILT, WHC, and Al – were shared among the top ten variables identified by models. Similar to trends observed in the GS and FST zones, increases in WHC, SILT, and Al were associated with reduced fertilizer effectiveness in the SDF zone. Additionally, in the SS zone, the use of briquette-form fertilizer application was associated with enhanced maize yield response, as indicated by the BRF model. However, this practice did not show a notable effect in the FST zone according to the same model.

3.4. Contribution of soil environment to fertilizer effect

Across the three methodological approaches used to evaluate fertil-

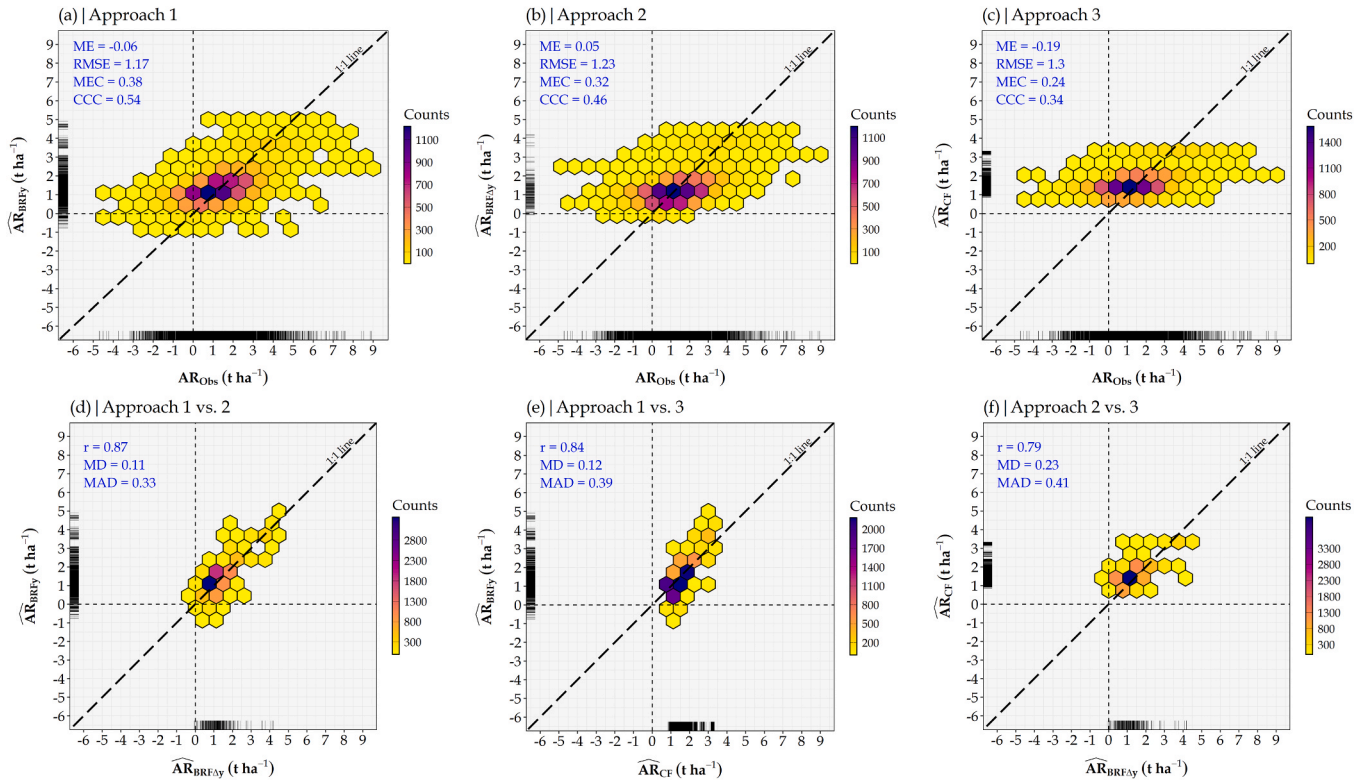

Fig. 2. Boosted random forest (BRF) and causal forest (CF) machine learning (ML) model evaluation based on the relationship between the observed absolute response (AR_{Obs}) and predicted fertilizer effect on maize grain yield and inter-model consistency in fertilizer effect predictions. Panels **(a)**, **(b)**, and **(c)** compare the AR_{Obs} to predicted fertilizer effect from the BRF in Approach 1 ($\widehat{AR}_{BRFy}$), BRF in Approach 2 ($\widehat{AR}_{BRF\Delta y}$), and CF in Approach 3 ($\widehat{AR}_{CF}$), respectively. Panels **(d)**, **(e)**, and **(f)** illustrate inter-model comparisons between predicted fertilizer effects: $\widehat{AR}_{BRFy}$ vs. $\widehat{AR}_{BRF\Delta y}$, $\widehat{AR}_{BRFy}$ vs. $\widehat{AR}_{CF}$, and $\widehat{AR}_{BRF\Delta y}$ vs. $\widehat{AR}_{CF}$. In each panel, the black dashed line represents the 1:1 line (perfect prediction and agreement). The grey bars at the left and the bottom side of each panel show the distribution of data points. The statistical metrics in blue were aggregated using the mean across the outer folds from the 10 × 10 nested cross-validation.

izer yield effects, both the CF and BRF models consistently identified SILT and Al as critical soil properties influencing fertilizer effectiveness. This finding aligns with earlier studies in Bindraban et al. (2015), Ouedraogo et al. (2020) and Sileshi et al. (2022), which emphasize the central role of soil properties in modulating crop responses to nutrient inputs. The SHAPDPs and ALE plots revealed that fertilizer contributed positively to maize grain yield when SILT content was below 18 % – with $\widehat{AR}_{BRFy}$ ranging from 141 kg ha^{-1} to 991 kg ha^{-1}, and $\widehat{AR}_{CF}$ ranging from 106 kg ha^{-1} to 134 kg ha^{-1}. However, this positive fertilizer effect diminished or reversed when SILT exceeded 18 %, as both models indicated negligible or no yield response to fertilizer in Approaches 1 and 3 (Fig. 5**a, c**). In Approach 2, the ALE plots did not exhibit a clear monotonic relationship between SILT and fertilizer effect (Fig. 5**b**). Nevertheless, the SHAPDP showed a negative trend, with positive fertilizer effects primarily observed when SILT was below 18 %. Similar findings were reported in Ichami et al. (2019) and Roobroeck et al. (2021) in Kenya and Nigeria, respectively, indicating that this response pattern may be widespread in sub-Saharan African (SSA) maize systems.

Soils exhibiting weak fertilizer responses are often described as "non-responsive soils" (Vanlauwe et al., 2010), where limited fertilizer effects arise either from inherently fertile soils or from local physical constraints that restrict plant access to nutrients (Kihara et al., 2016; Njoroge et al., 2017; Vanlauwe et al., 2023). One possible explanation is that soils with higher silt content may inherently supply more nutrients (Rex et al., 2021), thereby reducing the marginal benefit of additional fertilizer inputs. Another contributing factor may be the interaction between SILT and SMS. A moderate positive correlation was observed between SILT and SMS ($r = 0.38$, $p < 0.05$; Fig. S2), suggesting that higher silt levels are associated with increased moisture retention. In conditions where both SILT and SMS are elevated, excessive moisture may lead to poor soil aeration and root stress, thereby reducing fertilizer efficacy. Conversely, when SILT levels ranged from 10 % to 20 % – typical of sandy loam soils – and SMS ranged from 38 v% to 48 v% (Fig. 6**a, b, c**), the soil retained adequate moisture without becoming waterlogged. This condition allows for optimal root function and nutrient uptake, thus enhancing fertilizer effectiveness. This interpretation is further supported by findings in Iseki et al. (2023), who reported that spatial variability in cowpea (*Vigna unguiculata*) yield response to fertilizer in Burkina Faso was largely driven by excessive soil moisture content.

Furthermore, the 2D ALE plots for the SILT × CLAY interaction (Fig. S3) demonstrate that soil texture plays a pivotal role in yield response to fertilizer. Fertilizer effects were positive and pronounced in soils where SILT ranged from 18 % to 25 % and CLAY ranged from 10 % to 20 %. This specific range likely supports the optimal balance between nutrient retention (influenced by clay) and favorable physical conditions for root growth and aeration (influenced by silt and sand). Similar interactions have been observed in Argentina (Correndo et al., 2021), where soil texture modified the shape and magnitude of nitrogen response curves. These findings reinforce the importance of considering soil physical properties – alongside fertility indicators – when interpreting spatial variability in crop responses to fertilizer in smallholder systems (Pieri, 1992).

An increase in soil Al concentration was consistently associated with a reduction in fertilizer effectiveness, regardless of the modeling approach used or the AEZ considered (Figs. 3, 4, 5). SHAPDPs and ALE plots further illustrate a positive fertilizer response when soil Al levels were below 90–110 mg kg^{-1}, with estimated fertilizer effects ranging from 271 kg ha^{-1} to 626 kg ha^{-1} in Approach 1, from 38 kg ha^{-1} to 168 kg ha^{-1} in Approach 2, and from 212 kg ha^{-1} to 463 kg ha^{-1} in

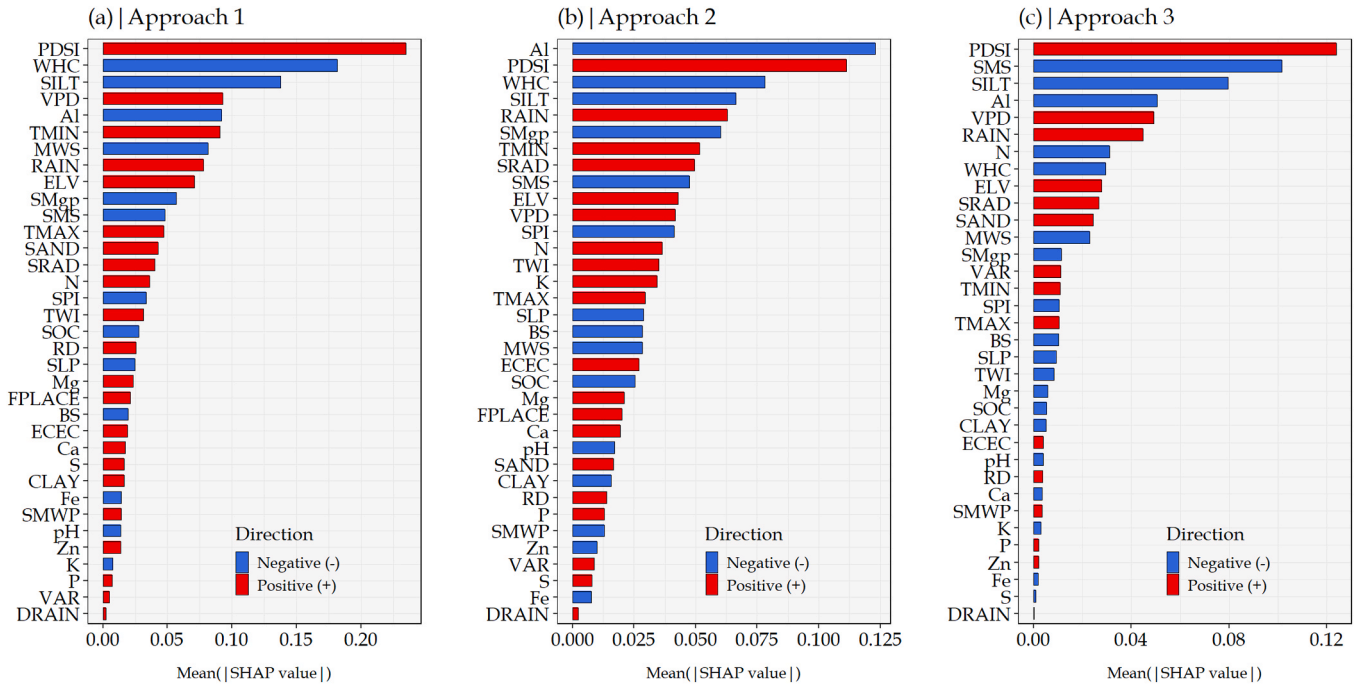

Fig. 3. Contributions of covariates to the variability in fertilizer-induced maize yield response in Ghana. Panels **(a)** and **(b)** present results from boosted random forest (BRF) models based on 10,916 observations under Approaches 1 and 2, respectively, while panel **(c)** shows results from a causal forest (CF) model using 2854 observations under Approach 3. The analyses utilize SHapley Additive exPlanations (SHAP) values to assess the relative importance of each covariate and the direction of their average contributions to the predicted fertilizer effects. In all panels, each bar represents the contribution of a covariate to the model's fertilizer effect prediction: red bars indicate positive average contributions, while blue bars indicate negative average contributions.

Approach 3 (Fig. 5 **a, b, c**). However, beyond this threshold Al = 90–110 mg kg^{-1}), the SHAP value and ALE curve declined sharply, ultimately resulting in negative yield responses. This finding might be explained by Al toxicity – a common occurrence in SSA acidic (pH < 7) (Table 1, Table S1 and S2), and phosphorus-depleted (5–12.5 mg kg^{-1}) soils (Table 1) (with optimal soil P for maize production in SSA > 25 mg kg^{-1}) – which can restrict crop root development and limit the uptake of essential nutrients such as P (Fageria and Baligar, 2008). In acidic soils, increased levels of exchangeable Al reduce P bioavailability; however, as soil pH rises, P is released and becomes accessible to plants. Consequently, the 2D ALE plot for the interaction between pH and Al showed a positive fertilizer effect when soil pH is increased from 5.3 to 6.4 and exchangeable Al is below 120 mg kg^{-1}, whereas low or no fertilizer effect is observed when soil pH is below 6 and exchangeable Al increases from 120 mg kg^{-1} to 210 mg kg^{-1} (Fig. 6**d, e, f**). These findings highlight the dual role of soil pH in controlling Al toxicity and P availability, underscoring how critical edaphic thresholds shape applied fertilizer effectiveness (Su et al., 2020).

3.5. *Climate-related heterogeneity of fertilizer effects*

Both the CF and BRF models identified VPD, RAIN, and PDSI as key climatic variables influencing the effectiveness of fertilizer on maize grain yield (Fig. 3). On average, higher VPD and PDSI values were associated with greater yield gains from fertilizer applications (Fig. 5**g, h, i, j, k, l**). The positive effects of fertilizer were especially pronounced in environments where growing season VPD ranged between 0.8 kPa and 1.4 kPa and PDSI values were between –2.0 and 1.9, indicative of moderately wet conditions. Conversely, in drier environments (i.e., PDSI ranging from –6.3 to –2.0), the contribution of fertilizer to maize yield was substantially reduced. For example, in experimental plots with PDSI values between –2.0 and 1.9, fertilizer-induced yield gains were substantial, ranging from 62 kg ha^{-1} to 1568 kg ha^{-1} in Approach 1.8 kg ha^{-1} to 463 kg ha^{-1} in Approach 2, and 166 kg ha^{-1} to 1119 kg ha^{-1} in Approach 3. These results are consistent with previous findings that highlight the suppressive effects of drought on fertilizer performance. Emery et al. (2020), for instance, reported that drought conditions significantly reduced NF efficacy in switchgrass (*Panicum virgatum*) in southwest Michigan, USA. Similarly, Juhász et al. (2024) showed that drought stress diminished S and N uptake in spring wheat (*Triticum aestivum L.*) in a controlled greenhouse experiment. The positive association between PDSI and fertilizer effectiveness can be attributed to improved moisture conditions in both the soil and atmosphere. PDSI was moderately correlated with RAIN ($r = 0.38$, $p < 0.05$) and growing-season soil moisture (SMgp; $r = 0.32$, $p < 0.05$). Rainfall itself was strongly correlated with SMgp ($r = 0.78$, $p < 0.05$) (Fig. S5). Interestingly, increases in SMgp were associated with reduced fertilizer effectiveness, possibly due to its negative correlation with RD ($r = -0.52$, $p < 0.05$), which may impair acquisition of nutrients from applied fertilizer. These findings underscore the critical role of water availability – not just quantity but also its interaction with root architecture – in modulating nutrient uptake (Li et al., 2009). As a well-established indicator of atmospheric drought, higher PDSI values reflect wetter conditions that enhance fertilizer dissolution and nutrient mobility via mass flow mechanisms (Swann et al., 2016).

In the VPD range of 0.8–1.5 kPa, fertilizer-induced yield responses increased from 81 kg ha^{-1} to 979 kg ha^{-1} according to BRF in Approach 1, from 30 kg ha^{-1} to 505 kg ha^{-1} according to BRF in Approach 2, and from 5 kg ha^{-1} to 141 kg ha^{-1} according to CF in Approach 3. This significant positive contribution of VPD to maize grain yield response under fertilization can be attributed to the balance between atmospheric moisture demand (driven by higher VPD) and soil moisture availability. As shown in Fig. 7, when VPD increased from 0.6 kPa to 1.2 kPa and SMgp ranged between 90 mm and 190 mm, fertilizer application enhanced maize grain yield by up to 20 kg ha^{-1} (CF) and 0.6–1.5 t ha^{-1} (BRF). By contrast, under drier conditions (SMgp < 90 mm), rising VPD did not translate into yield gains due to fertilizer application. These patterns can be explained mechanistically: under moderate to high soil moisture – maintained by sufficient rainfall – elevated VPD intensifies transpiration-driven mass flow, thereby facilitating nutrient dissolution

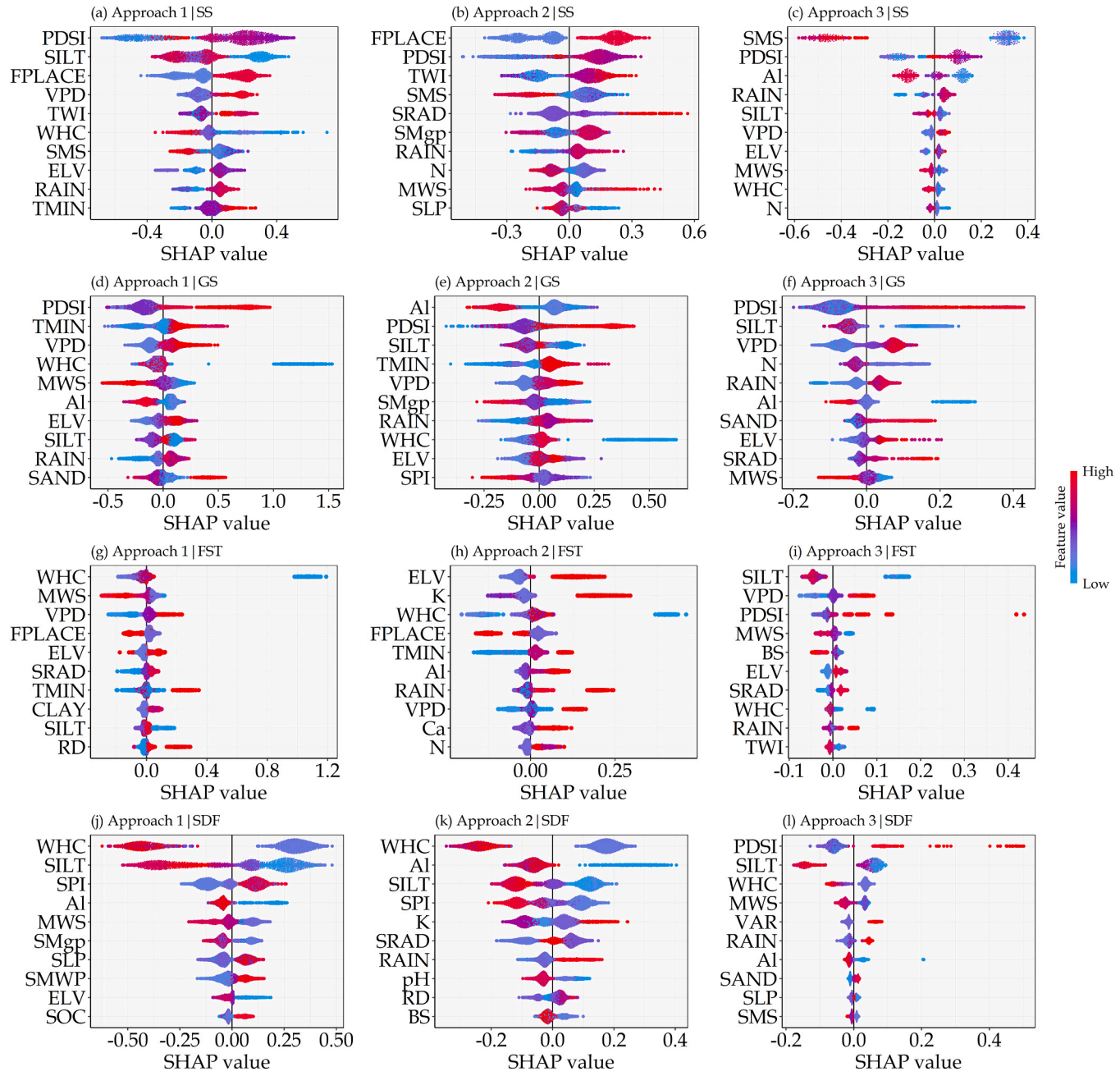

Fig. 4. SHapley Additive exPlanations (SHAP) summary plots showing the influence and importance of key covariates on fertilizer yield effect predictions across the four agroecological zones (AEZs) using causal forest (CF) and boosted random forest (BRF) models. AEZs include the **(a, b, c)** Sudan Savannah (SS); **(d, e, f)** Guinea Savannah (GS); **(g, h, i)** Forest-Savannah Transition (FST); and **(j, k, l)** Semi-Deciduous Forest (SDF). Each plot illustrates the ten most important covariates' individual SHAP values for each data point in the AEZ, i.e., the contribution of the ten most important covariates to fertilizer effect predictions (t ha^{-1}) according to the two machine learning models in Approaches 1, 2, and 3. The color represents the covariate value normalized in the range (0–1), with blue being low and red being high.

and uptake (Devi and Reddy, 2020). However, when soil moisture is limited, the heightened atmospheric demand imposed by increased VPD exacerbates water stress and undermines the crop's ability to mobilize and absorb applied nutrients from fertilizer.

Climate variables were among the most influential factors explaining the heterogeneity of fertilizer effects on maize yield across the SS, GS, and FST zones (Fig. 4). While the magnitude and direction of their contributions varied across AEZs, increases in seasonal RAIN, PDSI, and VPD were generally associated with positive fertilizer effect on maize grain yield. The SS zone exhibited the highest average and median fertilizer-induced yield gains (Table 3). This pronounced response can be attributed to a combination of favorable hydroclimatic conditions and inherent soil characteristics. During the maize growing season, the SS zone received substantial RAIN (~732 mm) and SRAD (~879.6 kWh m^{-2}) under moderate atmospheric demand (median VPD ≈ 1.0 kPa) (Tables S1 and S2). Together, these conditions promote photosynthesis, root growth, and nutrient uptake following fertilizer application. Moreover, the relatively low inherent soil fertility in the SS zone (Tables S1 and S2) likely amplified maize yield responses, as fertilizer inputs helped alleviate existing nutrient deficiencies. Hence, the combination of adequate water and energy inputs with fertilizer-induced nutrient correction explains the strong fertilizer efficacy observed in

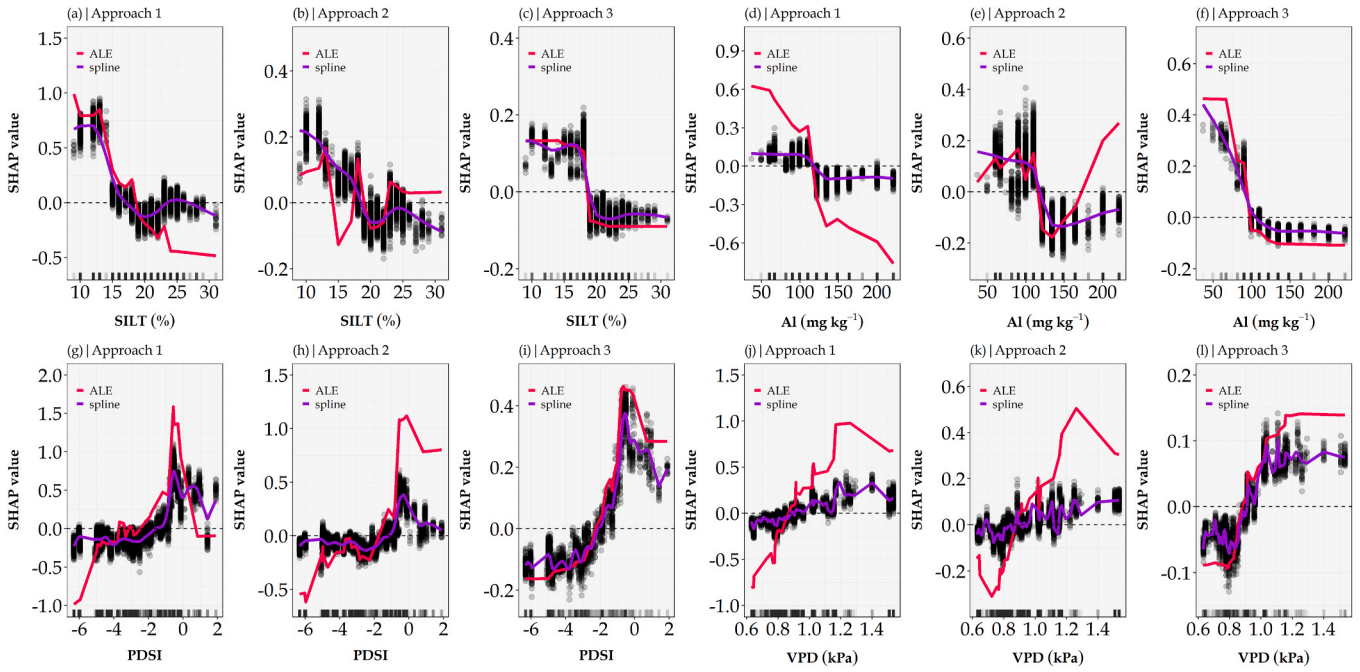

Fig. 5. Effect size of the four important covariates explaining fertilizer yield effect variability. Panels **(a-l)** show SHapley Additive exPlanations (SHAP) values (black dots) overlaid with accumulated local effects (ALE, red lines) and spline-smoothed trends regression fit to the SHAP values (purple lines) for **(a, b, c)** soil silt content (SILT, %); **(d, e, f)** soil exchangeable aluminum (Al, mg kg^{-1}); **(g, h, i)** Palmer Drought Severity Index (PDSI); and **(j, k, l)** vapor pressure deficit (VPD, kPa) from Approaches 1 and 2 (boosted random forest model) and Approach 3 (causal forest model). Marginal distributions of covariate values are visualized as grey density bars along the axes.

SS compared with other AEZs.

In contrast, within the more humid and inherently fertile SDF zone, the influence of climatic variables on the fertilizer effect, while still positive and significant, was secondary to that of soil properties. Soil physical characteristics (e.g., WHC, SILT) and chemical properties (e.g., Al) were the dominant factors modulating fertilizer response. This shift in driver importance occurs because, in humid and relatively fertile environments like SDF, water is less frequently the primary limiting factor. Consequently, fertilizer effects are predominantly governed by the soil's nutrient supply and retention capacity, a principle supported in Zingore et al. (2007), which demonstrated that low SOC led to poor fertilizer responses in Zimbabwe. Conversely, in the drier SS and GS zones, moisture availability strongly limits nutrient uptake, making climatic factors the predominant drivers of fertilizer responsiveness.

The critical influence of climate on fertilizer efficacy has direct implications for smallholder decision-making. Billé and Rogna (2021) and Heisse and Morimoto (2024) indicated that fertilizer adoption is highly sensitive to climate-related risks. Increased rainfall variability and warming could therefore undermine farmer confidence in fertilizer investments, particularly among capital-constrained smallholders, creating a cycle of low input use and poor yields. Similarly, Sileshi et al. (2008) attributed low fertilizer responsiveness in SSA to high interannual rainfall variability, while Ouedraogo et al. (2020) observed that yields of millet, sorghum, and maize increased with RAIN when fertilizer was applied. Overall, these results underscore that the interaction between hydroclimatic conditions and fertilizer responsiveness is highly AEZ-specific. Consequently, improving agronomic efficiency and reducing climate-related risks require nutrient management strategies tailored to AEZ moisture regimes. Key adaptations include adjusting fertilizer rates and application methods (e.g., FPLACE enhanced maize yield response in SS but not in FST) (Fig. 3 **a, b**), adopting moisture-conserving amendments, using drought-tolerant cultivars, and promoting integrated soil fertility management (Vanlauwe et al., 2015).

3.6. *Weaknesses, strengths and future work*

This study illustrates the capacity of ML models to estimate the causal effect of fertilizer on maize yield while uncovering the underlying sources of heterogeneity. These findings demonstrate the utility of causal ML in identifying key biophysical drivers of treatment effect variability, a critical step toward precision fertilizer management in SSA. Nonetheless, several methodological and contextual limitations should be acknowledged. A key limitation stems from the use of long-term static soil data. Although spatially detailed, these soil layers span nearly two decades, during which some properties may have changed due to land use dynamics, erosion, or management interventions. Such temporal mismatch could introduce or increase bias in model fertilizer effect estimates and prediction. Future studies would benefit from longitudinal soil sampling to better reflect current field conditions, though this is often constrained by logistical and financial challenges, particularly in resource-limited settings such as Ghana. In addition, the climate data used in this study may lack sufficient granularity due to the limited density of weather stations in Ghana (Kidd et al., 2017). This hampers the capacity to fully capture local climatic variability, especially for short-term or extreme weather events that strongly affect crop responses to fertilizer. Improving the resolution and accuracy of climate inputs would likely enhance model performance, but doing so would require infrastructural investments that extend beyond the scope of most agronomic studies.

Another methodological trade-off involves the dichotomization of treatment into fertilized versus control plots, considering only treatment plots meeting or exceeding minimum rate thresholds. While this binary approach streamlined statistical interpretation within a causal inference framework, it can mask the richness of dose-response relationships (Zhao et al., 2013). Moreover, this approach does not capture the variation in actual fertilizer rates applied by farmers, which are often far below the thresholds considered in this study, nor does it account for fertilizer application timing, a factor known to strongly influence fertilizer use efficiency (Mosisa et al., 2022). As a result, these limitations

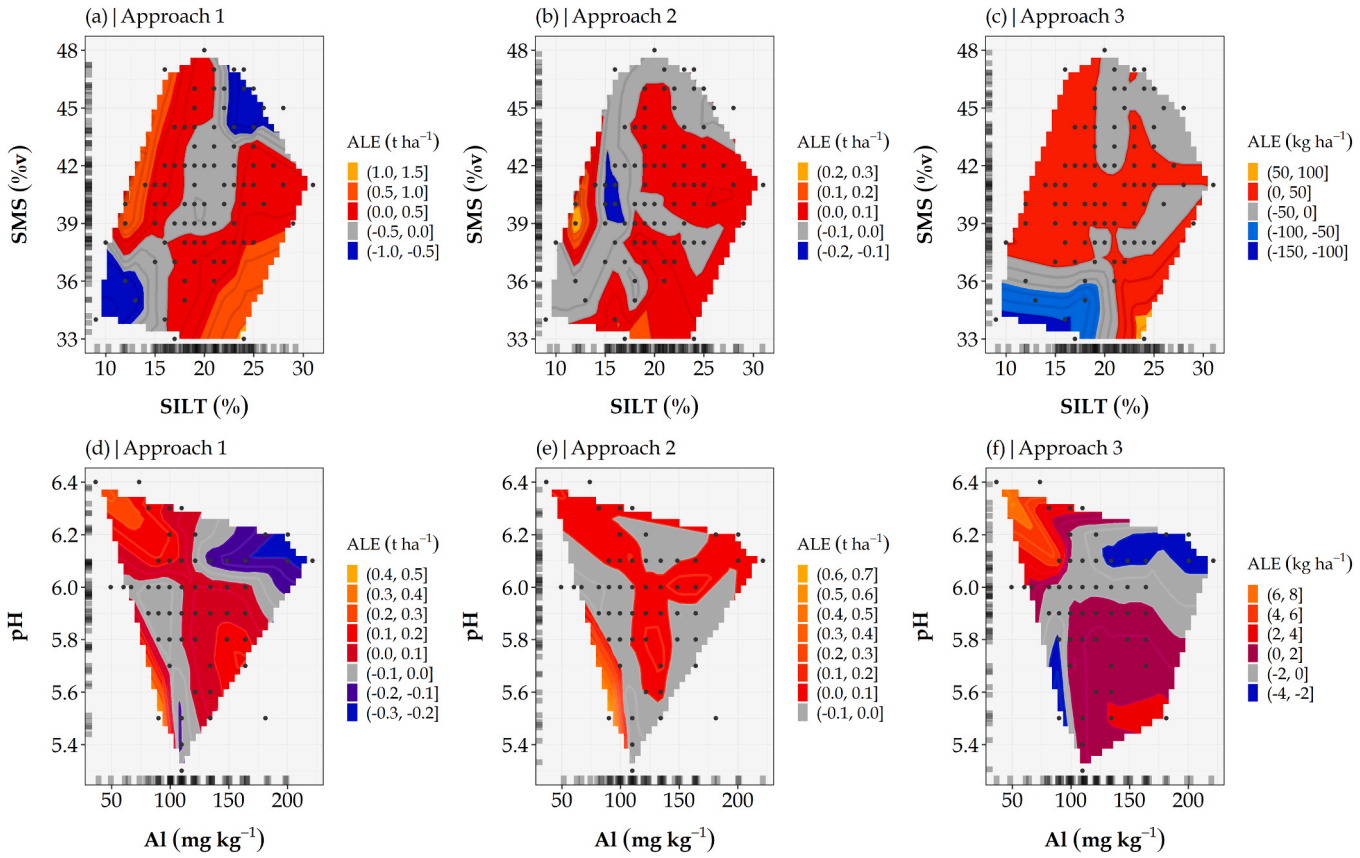

Fig. 6. Two-dimensional visualization of the contributions of the interactions between **(a, b, c)** soil silt content (SILT, %) and soil moisture content at saturation (SMS, %v) and **(d, e, f)** soil exchangeable aluminum (Al, mg kg^{-1}) and soil pH to predicted fertilizer effect. The color represents the accumulated local effect (ALE) values, with blue colors indicating negative interaction contribution to fertilizer effect and red to orange colors indicating positive interaction contribution. White-grey areas refer to covariate value combinations not present in the training dataset, where ALE values were not computed. The surface was obtained by bicubic interpolation of the ALE obtained from the calibration dataset. Marginal distributions of covariate values are visualized as grey density bars along the axes.

not only constrain the capacity to infer optimal input rates but also contribute to the unexplained portion of fertilizer effect variability. Emerging causal inference approaches that accommodate continuous treatment intensities, such as generalized propensity score models (Hirano and Imbens, 2004; Imai and Van Dyk, 2004), offer promising alternatives for future research.

The dataset was unbalanced; 63 % of observations came from the GS, and 71 % were collected between 2020 and 2022 (Fig. 1). This uneven distribution may have influenced how well the BRF and CF models generalized, as noted in Kowatsch et al. (2024). To limit this effect, we used weighting procedures during model training. Model performance varied across AEZs (Table S7). The highest model accuracies were observed in the SS, which had the fewest observations (Fig. 1**a**), with MEC values between 0.27 and 0.49. In contrast, performances were lowest in the FST zone. These differences reflect strong variation in soil and climate conditions that shape fertilizer responses. The weaker performances in the FST may be due to the higher CV in fertilizer effects (146.7 %) compared with 59.2 % in the SS (Table 3). In the SS, FPLACE improved fertilizer effect, while in the FST, fertilizer placement had little effect. This suggests that some management or environmental factors important for explaining fertilizer effect variability in the FST were not captured by the BRF and CF models. In this study, we did not pair weighting with stratified cross-validation nor did we evaluate the broader implications of spatiotemporal data imbalance on a model's capacity to generalize. Consequently, future work should use more advanced methods, such as spatiotemporal nested cross-validation, and systematic investigations into fertilizer effect prediction within imbalanced regression frameworks (Roberts et al., 2017; Sweet et al., 2023; Kamangir et al., 2024).

Understanding the spatial heterogeneity of yield response to fertilizers is essential for improving nutrient use efficiency in smallholder systems. Earlier studies (Sileshi et al., 2008, 2022; Kihara et al., 2016; Ouedraogo et al., 2020) reported this variability and related it to soil and climate conditions, though using mainly linear or meta-analytical approaches. More recent applications of ML (Abera et al., 2022; Zingore et al., 2022) improved predictive performance but remained correlative and did not isolate heterogeneous treatment effects. Kakimoto et al. (2022) demonstrated the potential of the CF model, albeit with synthetic data. Our study advances these works by applying a causal inference framework to extensive multi-year field data from Ghana, by combining CF with BRF models to support more context-specific fertilizer recommendations.

Further limitations arise from the controlled nature of the experimental data. Research-station trials, by design, exclude many confounding and collider factors encountered in real smallholder systems—such as pest outbreaks, labor constraints, and socio-economic variability. Consequently, the generalizability of these trial-based findings to farmer-managed conditions remains uncertain. Incorporating observational data from farmers' fields into CML frameworks could help address this gap, allowing for the estimation of fertilizer treatment effects under more realistic and heterogeneous conditions.

From a model interpretation standpoint, the study highlights notable differences in the consistency of ML interpretability tools. SHAPPDs and ALE curves yielded broadly aligned insights for the CF model, but less so for the BRF model (Fig. 5). This likely reflects the CF model's focus on stable, causally informative relationships, whereas classical ML models

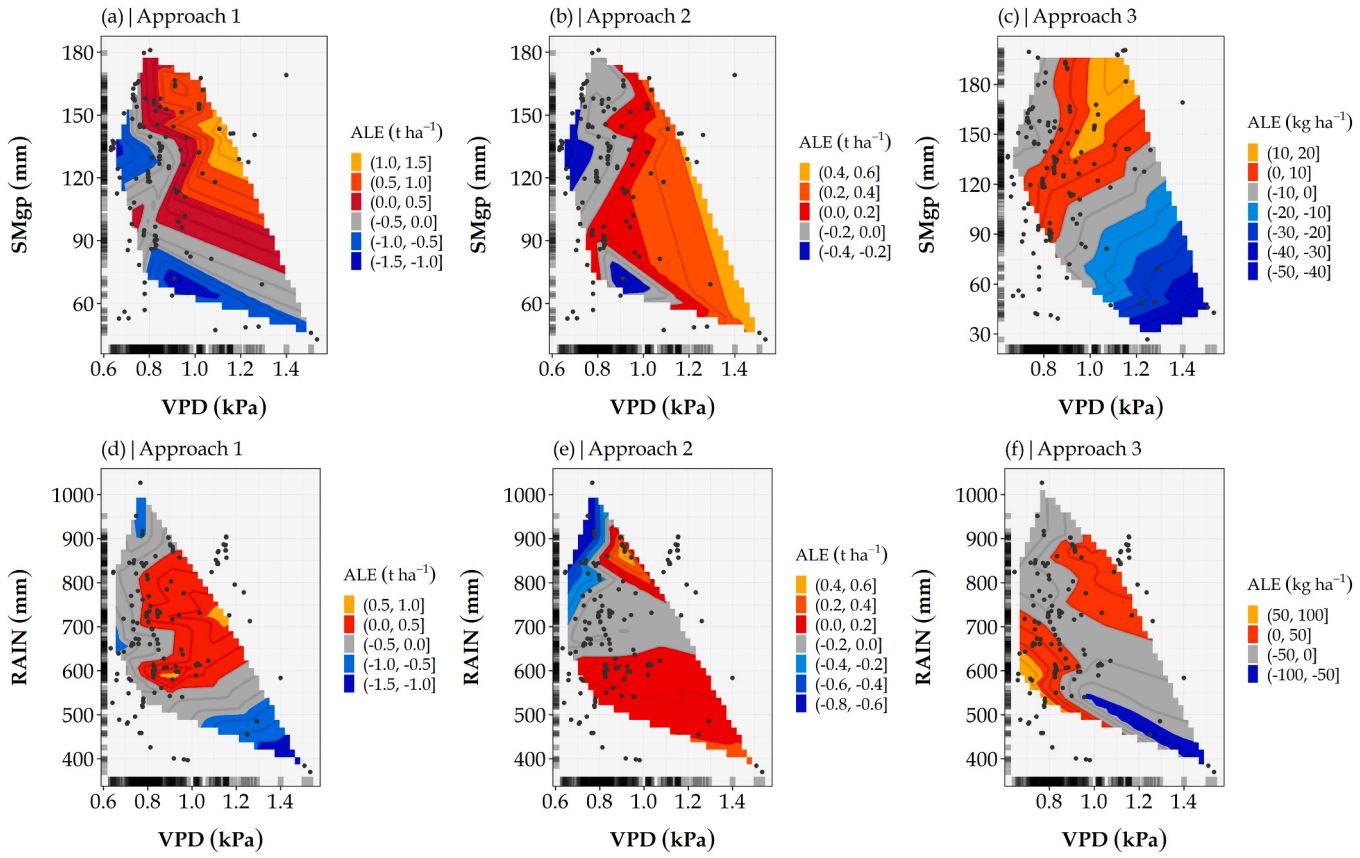

Fig. 7. Two-dimensional visualization of the contributions of the interactions between **(a, b, c)** vapor pressure deficit (VPD, kPa) and long-term soil moisture content (SMgp, mm) and **(d, e, f)** vapor pressure deficit (VPD, kPa) and cumulative rainfall (RAIN, mm) to predicted fertilizer effect. The color represents the accumulated local effect (ALE) values, with blue colors indicating negative interaction contribution to fertilizer effect and red to orange colors indicating positive interaction contribution. White-grey areas refer to covariate value combinations not present in the training dataset, where ALE values were not computed. The surface was obtained by bicubic interpolation of the ALE obtained from the calibration dataset. Marginal distributions of covariate values are visualized as grey density bars along the axes.

are more susceptible to confounding and noise. As such, CF not only supports causal inference but also improves transparency and interpretability – an advantage that is particularly relevant in data-driven agricultural policy and decision support systems. Despite the growing use of ML interpretability tools in predictive modeling, their application within causal ML remains limited (Svensson et al., 2025). This study contributes to a nascent yet critical area of research: interpretable causal modeling in agriculture. Further exploration of how interpretability methods interact with causal estimators will be vital for developing trustworthy, actionable recommendations in precision agronomy.

4. Conclusion

This study demonstrates the critical role of NPK fertilizer in enhancing maize grain yields across Ghana's AEZs while revealing substantial variability in fertilizer effects driven by soil, climate, topography, and management conditions. Using both predictive and causal ML models, we identified soil properties, particularly SILT, Al, and SMS, as major determinants of fertilizer responsiveness, alongside climatic factors such as RAIN, VPD, and PDSI. The fertilizer effect was strongest in the SS zone, where favorable hydroclimatic conditions and low inherent soil fertility enhanced yield responses to nutrient inputs. While BRF achieved high predictive accuracy, CF provided more interpretable causal relationships consistent with agronomic knowledge. The integration of predictive and causal ML thus offers a powerful framework for understanding site-specific variability in fertilizer effects and for supporting data-driven nutrient management strategies. Our findings argue against blanket fertilizer recommendations. Instead, they advocate for AEZ-specific guidelines that account for local soil and climate conditions. In climatically variable zones like the SS and GS, policies should promote weather-informed advisory systems and moisture-conserving practices to enhance returns on input investment and reduce farmer risk. To further improve the relevance of BRF and CF models, future work should incorporate dynamic soil data, continuous treatment levels, and on-farm observational data. Ultimately, this data-driven pathway toward site-specific recommendations can guide agricultural policy, optimize subsidy targeting, and support the resilience and livelihoods of Ghanaian farmers facing increasing climate uncertainty.

Declaration of Competing Interest

On behalf of all co-authors, I declare that there are no conflicts of interest related to this submission. This research was conducted under the Fertilizer Research and Responsible Implementation (FERARI) program, which is financially supported by the Université Mohammed VI Polytechnique, and the OCP Group.

Acknowledgments

We thank **Julie Kohler** and **Bethany Howard** of the International Fertilizer Development Center (IFDC) for their support in English language editing of the manuscript. This research was conducted using data generated under the Fertilizer Research and Responsible Implementation (FERARI) program. We gratefully acknowledge the financial support provided by Mohammed VI Polytechnic University and OCP group

to the FERARI program.

Appendix A. Supporting information

Supplementary data associated with this article can be found in the online version at doi:10.1016/j.fcr.2025.110287.

Data availability

Data will be made available on request.

References

Abatzoglou, J.T., Dobrowski, S.Z., Parks, S.A., Hegewisch, K.C., 2018. Terraclimate, a high-resolution global dataset of monthly climate and climatic water balance from 1958-2015. Sci. Data 5, 170191. https://doi.org/10.1038/sdata.2017.191.

Abera, W., Tamene, L., Tesfaye, K., Jiménez, D., Dorado, H., Erkossa, T., Kihara, J., Ahmed, J.S., Amede, T., Ramirez-Villegas, J., 2022. A data-mining approach for developing site-specific fertilizer response functions across the wheat-growing environments in Ethiopia. e9, Article e9 Exp. Agric. 58. https://doi.org/10.1017/S0014479722000047.

Apley, D.W., Zhu, J., 2020. Visualizing the effects of predictor variables in black box supervised learning models. J. R. Stat. Soc. Ser. B Stat. Methodol. 82 (4), 1059–1086. https://doi.org/10.1111/rssb.12377.

Athey, S., Imbens, G.W., Wager, S., 2018. Approximate residual balancing debiased inference of average treatment effects in high dimensions. J. R. Stat. Soc. Ser. B (Stat. Methodol.) 80 (4), 597–623. ⟨https://www.jstor.org/stable/26773172⟩.

Athey, S., Wager, S., 2019. Estimating treatment effects with causal forests: an application. Obs. Stud. 5 (2), 37–51. https://doi.org/10.1353/obs.2019.0001.

Bashagaluke, J.B., Logah, V., Opoku, A., Sarkodie-Addo, J., Quansah, C., 2018. Soil nutrient loss through erosion: Impact of different cropping systems and soil amendments in Ghana. PLoS One 13 (12), e0208250. https://doi.org/10.1371/journal.pone.0208250.

Bationo, A., Fening, J.O., and Kwaw, A. (2018). Assessment of Soil Fertility Status and Integrated Soil Fertility Management in Ghana. In A. Bationo, S. Youl, J. O. Fening, D. Ngaradoum, and F. Lompo (Eds.), Improving the Profitability, Sustainability and Efficiency of Nutrients Through Site Specific Fertilizer Recommendations in West Africa Agro-Ecosystems (Vol. 1, pp. 93-138). Springer International Publishing AG 2018. doi: 10.1007/978-3-319-58789-9_7.

Billé, A.G., Rogna, M., 2021. The effect of weather conditions on fertilizer applications: a spatial dynamic panel data analysis. J. R. Stat. Soc. Ser. A Stat. Soc. 185 (1), 3–36. https://doi.org/10.1111/rssa.12709.

Bindraban, P.S., Dimkpa, C., Nagarajan, L., Roy, A., Rabbinge, R., 2015. Revisiting fertilisers and fertilisation strategies for improved nutrient uptake by plants. Biol. Fertil. Soils 51 (8), 897–911. https://doi.org/10.1007/s00374-015-1039-7.

Boullouz, M., Bindraban, P.S., Kissiedu, I.N., Kouame, A.K.K., Devkota, K.P., Atakora, W. K., 2022. An integrative approach based on crop modeling and geospatial and statistical analysis to quantify and explain the maize (Zea mays) yield gap in Ghana. Front. Soil Sci. 2, 1037222. https://doi.org/10.3389/fsoil.2022.1037222.

Brandon, G., 2022. CRAN.package.fastshap, 10.32614/ fastshap Fast Approx. Shapley Values. https://doi.org/10.32614/CRAN.package.fastshap.

Bua, S., El-Mejahed, K., MacCarthy, D., Adogoba, D. S., Kissiedu, I. N., Atakora, W. K., Fosu, M., and S., B. P. (2020). *Yield responses of maize to fertilizers in Ghana* (FERARI Research Report No. 2), Issue. IFDC. https://ifdc.org/wp-content/uploads/2020/10/FERARI-Research-Report-2-Yield-Responses-of-Maize-to-Fertilizers-in-Ghana.pdf.

Caron, A., Baio, G., Manolopoulou, I., 2022. Shrinkage Bayesian Causal Forests for Heterogeneous Treatment Effects Estimation. J. Comput. Graph. Stat. 31 (4), 1202–1214. https://doi.org/10.1080/10618600.2022.2067549.

Chernozhukov, V., Chetverikov, D., Demirer, M., Duflo, E., Hansen, C., Newey, W., 2016. Double machine learning for treatment and causal parameters. mmap working paper, N ceo. CWP49/16, Centre for Microdata Methods and Practice (cemmap). doi:10.1920/wp.cem.2016.4916.

Correndo, A.A., Tremblay, N., Coulter, J.A., Ruiz-Diaz, D., Franzen, D., Nafziger, E., Prasad, V., Rosso, L.H.M., Steinke, K., Du, J., Messina, C.D., Ciampitti, I.A., 2021. Unraveling uncertainty drivers of the maize yield response to nitrogen: a Bayesian and machine learning approach. Agric. For. Meteorol. 311. https://doi.org/10.1016/j.agrformet.2021.108668.

Coulibali, Z., Cambouris, A.N., Parent, S.E., 2020. Site-specific machine learning predictive fertilization models for potato crops in Eastern Canada. PLoS One 15 (8), e0230888. https://doi.org/10.1371/journal.pone.0230888.

Dehghanisanij, H., Emami, S., Emami, H., Elbeltagi, A., 2024. Evaluating performance indicators of irrigation systems using swarm intelligence methods in Lake Urmia basin, Iran. Environ. Dev. Sustain. 26 (2), 4175–4195. https://doi.org/10.1007/s10668-022-02878-3.

Dehghanisanij, H., Emami, S., Rezaverdinejad, V., Amini, A., 2023. Potential of the hazelnut tree search–ELM hybrid approach in estimating yield and water productivity. Appl. Water Sci. 13 (2), 61. https://doi.org/10.1007/s13201-022-01865-3.

Deines, J.M., Wang, S., Lobell, D.B., 2019. Satellites reveal a small positive yield effect from conservation tillage across the US Corn Belt. Environ. Res. Lett. 14 (12). https://doi.org/10.1088/1748-9326/ab503b.

Devi, M.J., Reddy, V.R., 2020. Stomatal closure response to soil drying at different vapor pressure deficit conditions in maize. Plant Physiol. Biochem. 154, 714–722. https://doi.org/10.1016/j.plaphy.2020.07.023.

Dimkpa, C., Adzawla, W., Pandey, R., Atakora, W.K., Kouame, A.K.K., Jemo, M., Bindraban, P.S., 2023. Fertilizers for food and nutrition security in sub-Saharan Africa: An overview of soil health implications. Front. Soil Sci. 3. https://doi.org/10.3389/fsoil.2023.1123931.

Donkor, B., Bindraban, P.S., Simperegui, K.B.D., Kwesie, B., Kouame, A.K.K., Adzawla, W., 2025. Performance of LINTUL-2 in simulating water-limited yields of maize using different sets of weather data in Ghana, 10.1007/s10705-025-10422 Nutr. Cycl. Agroecosyst 8. https://doi.org/10.1007/s10705-025-10422-8.

Emery, S.M., Stahlheber, K.A., Gross, K.L., 2020. Drought minimized nitrogen fertilization effects on bioenergy feedstock quality. Biomass.. Bioenergy 133, 105452. https://doi.org/10.1016/j.biombioe.2019.105452.

Essel, B., Abaidoo, R.C., Opoku, A., Ewusi-Mensah, N., 2020. Economically optimal rate for nutrient application to maize in the semi-deciduous forest zone of Ghana. J. Soil Sci. Plant Nutr. 20 (4), 1703–1713. https://doi.org/10.1007/s42729-020-00240-y.

Fageria, N.K., Baligar, V.C., 2008. Ameliorating Soil acidity of tropical oxisols by liming for sustainable crop production. In (10.1016/s0065-2113(08)00407-0pp., 345–399. doi:10.1016/s0065-2113(08)00407-0.

Falconnier, G.N., Cardinael, R., Corbeels, M., Baudron, F., Chivenge, P., Couëdel, A., Ripoche, A., Affholder, F., Naudin, K., Benaillon, E., Rusinamhodzi, L., Leroux, L., Vanlauwe, B., Giller, K.E., 2023. The input reduction principle of agroecology is wrong when it comes to mineral fertilizer use in sub-Saharan Africa. Outlook Agric., 10.1177/00307270231199795 https://doi.org/10.1177/00307270231199795.

Farr, T.G., Rosen, P.A., Caro, E., Crippen, R., Duren, R., Hensley, S., Kobrick, M., Paller, M., Rodriguez, E., Roth, L., Seal, D., Shaffer, S., Shimada, J., Umland, J., Werner, M., Oskin, M., Burbank, D., Alsdorf, D.E., 2007. The shuttle radar topography mission. Reviews of Geophysics 45, RG2004. https://doi.org/10.1029/2005RG000183.

Feuerriegel, S., Frauen, D., Melnychuk, V., Schweisthal, J., Hess, K., Curth, A., Bauer, S., Kilbertus, N., Kohane, I.S., van der Schaar, M., 2024. Causal machine learning for predicting treatment outcomes. Nat. Med 30 (4), 958–968. https://doi.org/10.1038/s41591-024-02902-1.

Fisher, R.A., 1992. In: Kotz, S., Johnson, N. L. (Eds.). In: Breakthroughs in Statistics: Methodology and Distribution, (10.1007/978-1-4612-4380-9_6pp. Springer, New York, pp. 66–70. doi:10.1007/978-1-4612-4380-9_6.

Friedman, J.H., 2001. Greedy function approximation: a gradient boosting machine. Ann. Stat. 29 (5), 1189–1232. https://doi.org/10.1214/aos/1013203451.

Ghosal, I., Hooker, G., 2020. Boosting Random Forests to Reduce Bias; One-Step Boosted Forest and Its Variance Estimate. J. Comput. Graph. Stat. 30 (2), 493–502. https://doi.org/10.1080/10618600.2020.1820345.

Heerwaarden, v J., Ronner, E., Baijukya, F., Adjei-Nsiah, S., Ebanyat, P., Kamai, N., Wolde-meskel, E., Vanlauwe, B., Giller, K.E., 2023. Consistency, variability, and predictability of on-farm nutrient responses in four grain legumes across East and West Africa. Field Crops Res. 299. https://doi.org/10.1016/j.fcr.2023.108975.

Heisse, C., Morimoto, R., 2024. Climate vulnerability and fertilizer use – panel evidence from Tanzanian maize farmers. Clim. Dev. 16 (3), 242–254. https://doi.org/10.1080/17565529.2023.2206373.

Hersbach, H., Bell, B., Berrisford, P., 2020. The ERA5 global reanalysis. Q. J. R. Meteorol. Soc. 146 (730), 1999–2049. https://doi.org/10.1002/qj.3803.

Hijmans, R.J., Bivand, R., Forner, K., Ooms, J., Pebesma, E., and Sumner, M.D. (2022). terra: Spatial Data Analysis. https://cran.r-project.org/web/packages/terra/index.html.

Hirano, K., Imbens, G.W., 2004. In: Shewhart, W.A., Wilks, S.S., Gelman, A., Meng, X.-L. (Eds.), Applied Bayesian Modeling and Causal Inference from Incomplete-Data Perspectives. John Wiley & Sons Ltd., pp. 73–84. https://doi.org/10.1002/0470090456.ch7

Holland, P.W., 1986. Statistics and Causal Inference. J. Am. Stat. Assoc. 81 (396), 945–960. https://doi.org/10.2307/2289064.

Ichami, S.M., Shepherd, K.D., Sila, A.M., Stoorvogel, J.J., Hoffland, E., 2019. Fertilizer response and nitrogen use efficiency in African smallholder maize farms. Nutr. Cycl. Agroecosyst 113 (1), 1–19. https://doi.org/10.1007/s10705-018-9958-y.

Imai, K., Van Dyk, D.A., 2004. Causal inference with general treatment regimes: Generalizing the propensity score. J. Am. Stat. Assoc. 99 (467), 854–866. https://doi.org/10.1198/016214504000001187.

Imbens, G.W., Rubin, D.B., 2015. *Causal Inference for Statistics, Social, and Biomedical Sciences: An Introduction*. Cambridge University Press. https://doi.org/10.1017/CBO9781139025751.

Iseki, K., Ikazaki, K., Batieno, B.J., 2023. Heterogeneity effects of plant density and fertilizer application on cowpea grain yield in soil types with different physicochemical characteristics. Field Crops Res. 292, 108825. https://doi.org/10.1016/j.fcr.2023.108825.

Jakobsen, K.D., 2023. RE: "Practical Guide to Honest Causal Forests for Identifying Heterogeneous Treatment Effects. Am. J. Epidemiol. 193 (5), 811–812. https://doi.org/10.1093/aje/kwad147.

Juhász, E.K., Kremper, R., Tállai, M., Béni, Á., Novák, T., Kovács, A.B., 2024. Evaluation of the Effects of Drought Stress and Nitrogen-Sulfur Fertilization on Productivity and Yield Parameters of Spring Wheat. Stresses 4 (4), 850–859. https://doi.org/10.3390/stresses4040056.

Kakimoto, S., Mieno, T., Tanaka, T.S.T., Bullock, D.S., 2022. Causal forest approach for site-specific input management via on-farm precision experimentation. Comput. Electron. Agric. 199. https://doi.org/10.1016/j.compag.2022.107164.

Kamangir, H., Sams, B.S., Dokoozlian, N., Sanchez, L., Earles, J.M., 2024. Large-scale spatio-temporal yield estimation via deep learning using satellite and management

data fusion in vineyards. Comput. Electron. Agric. 216. https://doi.org/10.1016/j.compag.2023.108439.
Kidd, C., Becker, A., Huffman, G.J., Muller, C.L., Joe, P., Skofronick-Jackson, G., Kirschbaum, D.B., 2017. So, How Much of the Earth's Surface Is Covered by Rain Gauges? Bull. Amer. Meteorol. Soc. 98 (1), 69–78. https://doi.org/10.1175/BAMS-D-14-00283.1.
Kihara, J., Nziguheba, G., Zingore, S., Coulibaly, A., Esilaba, A., Kabambe, V., Njoroge, S., Palm, C., Huising, J., 2016. Understanding variability in crop response to fertilizer and amendments in sub-Saharan Africa. Agric. Ecosyst. Environ. 229, 1–12. https://doi.org/10.1016/j.agee.2016.05.012.
Kluger, D.M., Owen, A.B., Lobell, D.B., 2022. Combining randomized field experiments with observational satellite data to assess the benefits of crop rotations on yields. Environ. Res. Lett. 17 (4), 044066. https://doi.org/10.1088/1748-9326/ac6083.
Kouame, A.K.K., Bindraban, P.S., Jallal, L., Kwesie, B., Anokye, A.N.A.F., El Allali, A., Adzawla, W., 2025b. Effect of sulfur- and zinc-containing fertilizers on soybean yield and analysis of spatial and seasonal yield variability in Ghana, West Africa. Eur. J. Agron. 164. https://doi.org/10.1016/j.eja.2024.127461.
Kouame, A.K.K., Bindraban, P.S., Kissiedu, I.N., Atakora, W.K., El Mejahed, K., 2023. Identifying drivers for variability in maize (Zea mays L.) yield in Ghana: A meta-regression approach. Agric. Syst. 209. https://doi.org/10.1016/j.agsy.2023.103667.
Kouame, A.K.K., Heuvelink, G.B.M., Bindraban, P.S., 2025a. Unraveling drivers of maize (Zea mays L.) yield variability in Ghana: A machine learning approach. Comput. Electron. Agric. 237. https://doi.org/10.1016/j.compag.2025.110647.
Kowatsch, D., Müller, N.M., Tscharke, K., Sperl, P., and Bötinger, K. (2024). Imbalance in Regression Datasets. *arXiv*, ⟨https://arxiv.org/abs/2402.11963⟩.
Krstajic, D., Buturovic, L.J., Leahy, D.E., Thomas, S., 2014. Cross-validation pitfalls when selecting and assessing regression and classification models. J. Chemin.. 6 (1), 10. https://doi.org/10.1186/1758-2946-6-10.
Kuhn, M., 2008. Building predictive models in R using the caret package. J. Stat. Softw. 28, 1–26. https://doi.org/10.18637/jss.v028.i05.
Lewis, M.J., Spiliopoulou, A., Goldmann, K., Pitzalis, C., McKeigue, P., Barnes, M.R., 2023. nestedcv: an R package for fast implementation of nested cross-validation with embedded feature selection designed for transcriptomics and high-dimensional data. Bioinform Adv. 3 (1), vbad048. https://doi.org/10.1093/bioadv/vbad048.
Li, S.X., Wang, Z.H., Malhi, S.S., Li, S.Q., Gao, Y.J., Tian, X.H., 2009. Nutrient and Water Management Effects on Crop Production, and Nutrient and Water Use Efficiency in Dryland Areas of China. In: Advances in Agronomy, 102. Academic Press, pp. 223–265. https://doi.org/10.1016/S0065-2113(09)01007-4.
Lin, L.I., 1989. A concordance correlation coefficient to evaluate reproducibility, 10.2307/2532051 Biometrics 45, 255–268. https://doi.org/10.2307/2532051.
Lundberg, S.M., and Su-In, L. (2017). A unified approach to interpreting model predictions Proceedings of the 31st International Conference on Neural Information Processing Systems, Long Beach, California, USA. ⟨https://dl.acm.org/doi/10.5555/3295222.3295230⟩.
Moccia, C., Moirano, G., Popovic, M., Pizzi, C., Fariselli, P., Richiardi, L., Ekstrom, C.T., Maule, M., 2024. Machine learning in causal inference for epidemiology. Eur. J. Epidemiol. 39 (10), 1097–1108. https://doi.org/10.1007/s10654-024-01173-x.
Molnar, C., Casalicchio, G., Bischl, B., 2018. iml: An R package for Interpretable Machine Learning. J. Open Source Softw. 3 (26), 786. https://doi.org/10.21105/joss.00786.
Molnar, C., 2025. Interpretable Machine Learning: A Guide for Making Black Box Models Explainable, 3 ed. https://christophm.github.io/interpretable-ml-book.
Mosisa, W., Dechassa, N., Kibret, K., Zeleke, H., Bekeko, Z., 2022. Effects of timing and nitrogen fertilizer application rates on maize yield components and yield in eastern Ethiopia. Agrosystems Geosci. Environ. 5 (4), e20322. https://doi.org/10.1002/agg2.20322.
Nash, J.E., Sutcliffe, J.V., 1970. River flow forecasting through conceptual models part I–A discussion of principles. J. Hydrol. 10 (3), 282–290. https://doi.org/10.1016/0022-1694(70)90255-6.
Njoroge, R., Otinga, A.N., Okalebo, J.R., Pepela, M., Merckx, R., 2017. Occurrence of poorly responsive soils in western Kenya and associated nutrient imbalances in maize (Zea mays L.). Field Crops Res. 210, 162–174. https://doi.org/10.1016/j.fcr.2017.05.015.
Nziguheba, G., van Heerwaarden, J., Vanlauwe, B., 2021. Quantifying the prevalence of (non)-response to fertilizers in sub-Saharan Africa using on-farm trial data. Nutr. Cycl. Agroecosystems 121 (2-3), 257–269. https://doi.org/10.1007/s10705-021-10174-1.
Ouedraogo, Y., Taonda, J.B.S., Sermé, I., Tychon, B., Bielders, C.L., 2020. Factors driving cereal response to fertilizer microdosing in sub-Saharan Africa: A meta-analysis. Agron. J. 112 (4), 2418–2431. https://doi.org/10.1002/agj2.20229.
Palmer, W.C. (1965). Meteorological drought. Research Paper no. 45. washington, DC: US department of commerce. Weather Bureau, pp. 59., ⟨https://www.ncei.noaa.gov/monitoring-content/temp-and-precip/drought/docs/palmer.pdf⟩.
Penuelas, J., Coello, F., Sardans, J., 2023. A better use of fertilizers is needed for global food security and environmental sustainability. Agric. Food Secur. 12 (1), 5. https://doi.org/10.1186/s40066-023-00409-5.
Pieri, C.J.M.G. (1992). Fertility of soils: a future for farming in the West African Savannah (Vol. 10). Springer Berlin, Heidelberg. https://doi.org/10.1007/978-3-642-84320-4.
Poggio, L., De Sousa, L.M., Batjes, N.H., Heuvelink, G., Kempen, B., Ribeiro, E., Rossiter, D., 2021. 2.0: producing soil information for the globe with quantified spatial uncertainty. *SOIL*. Soil Grids 7 (1), 217–240. https://doi.org/10.5194/soil-7-217-2021.
R Core Team (2025). R: A language and environment for statistical computing. R Foundation for Statistical Computing, Vienna, Austria. ⟨https://www.R-project.org/.⟩.
Rex, D., Clough, T.J., Lanigan, G.J., Jansen-Willems, A.B., Condron, L.M., Richards, K.G., Müller, C., 2021. Gross N transformations vary with soil moisture and time following urea deposition to a pasture soil. Geoderma 386, 114904. https://doi.org/10.1016/j.geoderma.2020.114904.
Roberts, D.R., Bahn, V., Ciuti, S., Boyce, M.S., Elith, J., Guillera-Arroita, G., Hauenstein, S., Lahoz-Monfort, J.J., Schröder, B., Thuiller, W., 2017. Cross-validation strategies for data with temporal, spatial, hierarchical, or phylogenetic structure. Ecography 40 (8), 913–929. https://doi.org/10.1111/ecog.02881.
Röhrig, F., Lange, S., Aschenbrenner, P., Chemura, A., Murken, L., Grams, E., Klockemann, L., Romanato, E., Haider, J., and Gornot, C. (2019). Climate Risk Profile for Ghana. A joint publication by the Potsdam Institute for Climate Impact Research, the German Federal Ministry for Economic Cooperation and Development, the Deutsche Gesellschaft für Internationale Zusammenarbeit GmbH and the KfW Development Bank, 12 pp. https://www.pik-potsdam.de/members/gornott/climate-risk-profile-ghana.pdf.
Ronner, E., Franke, A.C., Vanlauwe, B., Dianda, M., Edeh, E., Ukem, B., Bala, A., van Heerwaarden, J., Giller, K.E., 2016. Understanding variability in soybean yield and response to P-fertilizer and rhizobium inoculants on farmers' fields in northern Nigeria. Field Crops Res. 186, 133–145. https://doi.org/10.1016/j.fcr.2015.10.023.
Roobroeck, D., Palm, C.A., Nziguheba, G., Weil, R., Vanlauwe, B., 2021. Assessing and understanding non-responsiveness of maize and soybean to fertilizer applications in African smallholder farms. Agric. Ecosyst. Environ. 305, 107165. https://doi.org/10.1016/j.agee.2020.107165.
Rosenblatt, M., Tejavibulya, L., Jiang, R., Noble, S., Scheinost, D., 2024. Data leakage inflates prediction performance in connectome-based machine learning models. Nat. Commun. 15 (1), 1829. https://doi.org/10.1038/s41467-024-46150-w.
Rubin, D.B., 1974. Estimating Causal Effects of Treatments in Randomized and Nonrandomized Studies. J. Educ. Psychol. 66 (5), 688–701. https://doi.org/10.1037/h0037350.
Shapley, L.S., 1953. A Value for n-Person Games. In: Kuhn, H.W., Tucker, A.W. (Eds.), Contributions to the Theory of Games (AM-28) Volume II. Princeton University Press, pp. 307–317. https://doi.org/10.1515/9781400881970-018.
Sileshi, G.W., Akinnifesi, F.K., Ajayi, O.C., Place, F., 2008. Meta-analysis of maize yield response to woody and herbaceous legumes in sub-Saharan Africa. Plant Soil 307 (1), 1–19. https://doi.org/10.1007/s11104-008-9547-y.
Sileshi, G.W., Kihara, J., Tamene, L., Vanlauwe, B., Phiri, E., Jama, B., 2022. Unravelling causes of poor crop response to applied N and P fertilizers on African soils. Exp. Agric. 1–17. https://doi.org/10.1017/S0014479721000247.
Simperegui, K.B.D., Bindraban, P.S., Kouame, A.K.K., Peluffo-Ordóñez, D.H., and Atakora, W.K. (2023). Estimation of water-limited maize yield using the LINTUL-2 model and spatial analysis of the yield gap in Ghana (FERARI Research Report No. 13), Issue. IFDC. https://api.hub.ifdc.org/server/api/core/bitstreams/85dcecbf-7c6f-43d2-abf1-5fbcb524debb/content.
Splawa-Neyman, J., 1923. In: Sur les Applications de la Théorie des Probabilités aux Experiences Agricoles: Essai des Principes, 10. Roczniki Nauk Rolniczych, pp. 1–51. https://typeset.io/pdf/on-the-application-of-probability-theory-to-agricultural-4ynt7v0y35.pdf.
SRID/MoFA. (2021). *Agriculture in Ghana: Facts and Figures (2020)*. https://srid.mofa.gov.gh/sites/default/files/Agriculture%20In%20Ghana%20Facts%20%26%20Figures_%202020%20FINAL.pdf.
Stetter, C., and Sauer, J. (2021). Exploring the heterogeneous effects of weather on productivity using generalized random forests, 95th Annual Conference, March 29-30, 2021, Warwick, UK (Hybrid) 312074, Agricultural Economics Society - AES. doi: 10.22004/ag.econ.312074.
Su, W., Ahmad, S., Ahmad, I., Han, Q., 2020. Nitrogen fertilization affects maize grain yield through regulating nitrogen uptake, radiation and water use efficiency, photosynthesis and root distribution. PeerJ 8, e10291. https://doi.org/10.7717/peerj.10291.
Svensson, D., Hermansson, E., Nikolaou, N., Sechidis, K., Lipkovich, I., 2025. arXiv preprint. Overv. Pract. Recomm. Using Shapley Values identifying Predict. Biomark. via CATE Model. ⟨https://arxiv.org/pdf/2505.01145⟩.
Swann, A.L., Hoffman, F.M., Koven, C.D., Randerson, J.T., 2016. Plant responses to increasing CO2 reduce estimates of climate impacts on drought severity. Proc. Natl. Acad. Sci. USA 113 (36), 10019–10024. https://doi.org/10.1073/pnas.1604581113.
Sweet, L. b, Müller, C., Anand, M., Zscheischler, J., 2023. Cross-Validation Strategy Impacts the Performance and Interpretation of Machine Learning Models. Artif. Intell. Earth Syst. 2 (4), e230026. https://doi.org/10.1175/AIES-D-23-0026.1.
Tanaka, T.S.T., Heuvelink, G.B.M., Mieno, T., Bullock, D.S., 2024. Can machine learning models provide accurate fertilizer recommendations?, 10.1007/s11119-024-10136-x Precis. Agric.. https://doi.org/10.1007/s11119-024-10136-x.
Tetteh, F.M., Ennim, S.A., Issaka, R.N., Buri, M., Ahiabor, B.A.K., Fening, J.O., 2018. Fertilizer Recommendation for Maize and Cassava Within the Breadbasket Zone of Ghana. In: Bationo, In.A., Ngaradoum, D., Youl, S., Lompo, F., Fening, J.O. (Eds.), Improving the Profitability, Sustainability and Efficiency of Nutrients Through Site Specific Fertilizer Recommendations in West Africa Agro-Ecosystems, pp. 161–184. https://doi.org/10.1007/978-3-319-58792-9_10.
Tetteh, F.M., Quansah, G.W., Frempong, S.O., Nurudeen, A.R., Atakora, W.K., and Opoku, G. (2017). Optimizing fertilizer use within the context of integrated soil fertility management in Ghana. In C. S. Wortmann and K. Sones (Eds.), Fertilizer Use Optimization in Sub-Saharan Africa (pp. 67-81). CAB International.
Thorburn, P.J., Biggs, J.S., Puntel, L.A., Sawyer, J.E., Everingham, Y.L., Archontoulis, S. V., 2024. The nitrogen fertilizer conundrum: why is yield a poor determinant of crops' nitrogen fertilizer requirements? Agron. Sustain. Dev. 44 (2), 18. https://doi.org/10.1007/s13593-024-00955-7.

Tibshirani, J., Athey, S., Friedberg, R., Hadad, V., Hirshberg, D., Miner, L., Sverdrup, E., Wager, S., Wright, M., 2024. grf Gen. Random For. 1–89. https://doi.org/10.32614/CRAN.package.grf, 10.32614/CRAN.package.grf,.

Tsoumas, I., Giannarakis, G., Sitokonstantinou, V., Koukos, A., Loka, D., Bartsotas, N., Kontoes, C., Athanasiadis, I., 2023. Evaluating digital agriculture recommendations with causal inference. Proc. AAAI Conf. Artif. Intell. 37 (12), 14514–14522. https://doi.org/10.1609/aaai.v37i12.26697.

Turek, M.E., Poggio, L., Batjes, N.H., Armindo, R.A., de Jong van Lier, Q., de Sousa, L.M., Heuvelink, G.B.M., 2023. Global mapping of volumetric water retention at 100, 330 and 15000 cm suction using the WoSIS database. Int. Soil Water Conserv. Res. 11 (2), 225–239. https://doi.org/10.1016/j.iswcr.2022.08.001.

Uwiragiye, Y., Junior Yannick Ngaba, M., Zhao, M., Elrys, A.S., Heuvelink, G.B.M., Zhou, J., 2022. Modelling and mapping soil nutrient depletion in humid highlands of East Africa using ensemble machine learning: A case study from Rwanda. CATENA 217, 106499. https://doi.org/10.1016/j.catena.2022.106499.

Vanlauwe, B., Amede, T., Bationo, A., Bindraban, P., Breman, H., Cardinael, R., Couedel, A., Chivenge, P., Corbeels, M., Dobermann, A., Falconnier, G., Fatunbi, W., Giller, K., Harawa, R., Kamau, M., Merckx, R., Palm, C., Powlson, D., Rusinamhodzi, L., … Groot, R. (2023). Fertilizer and soil health in Africa: The role of fertilizer in building soil health to sustain farming and address climate change. https://ifdc.org/wp-content/uploads/2023/02/Fertilizer-and-Soil-Health-in-Africa-The-Role-of-Fertilizer-in-Building-Soil-Health-to-Sustain-Farming-and-Address-Climate-Change.pdf.

Vanlauwe, B., Bationo, A., Chianu, J., Giller, K.E., Merckx, R., Mokwunye, U., Ohiokpehai, O., Pypers, P., Tabo, R., Shepherd, K.D., Smaling, E.M.A., Woomer, P.L., Sanginga, N., 2010. Integrated soil fertility management:operational definition and consequences for implementation and dissemination. Outlook Agric. 39 (1), 17–24. https://doi.org/10.5367/000000010791169998.

Vanlauwe, B., Descheemaeker, K., Giller, K.E., Huising, J., Merckx, R., Nziguheba, G., Wendt, J., Zingore, S., 2015. Integrated soil fertility management in sub-Saharan Africa: unravelling local adaptation. SOIL 1 (1), 491–508. https://doi.org/10.5194/soil-1-491-2015.

Venkatasubramaniam, A., Mateen, B.A., Shields, B.M., Hattersley, A.T., Jones, A.G., Vollmer, S.J., Dennis, J.M., 2023. Comparison of causal forest and regression-based approaches to evaluate treatment effect heterogeneity: an application for type 2 diabetes precision medicine. BMC Med Inf. Decis. Mak. 23 (1), 110. https://doi.org/10.1186/s12911-023-02207-2.

Wager, S., Athey, S., 2018. Estimation and inference of heterogeneous treatment effects using random forests. J. Am. Stat. Assoc. 113 (523), 1228–1242. https://doi.org/10.1080/01621459.2017.1319839.

Yamba, E.I., Aryee, J.N.A., Quansah, E., Davies, P., Wemegah, C.S., Osei, M.A., Ahiataku, M.A., Amekudzi, L.K., 2023. Revisiting the agro-climatic zones of Ghana: a re-classification in conformity with climate change and variability. PLOS Clim. 2 (1), e0000023. https://doi.org/10.1371/journal.pclm.0000023.

Young, H.P., 1985. Monotonic solutions of cooperative games. Int. J. Game Theory 14 (2), 65–72. https://doi.org/10.1007/bf01769885.

Zhao, S., Van Dyk, D.A., Imai, K., 2013. Causal Inference Obs. Stud. NonBin. Treat. arXiv Prepr. ⟨https://arxiv.org/pdf/1309.6361⟩.

Zingore, S., Adolwa, I.S., Njoroge, S., Johnson, J.M., Saito, K., Phillips, S., Kihara, J., Mutegi, J., Murell, S., Dutta, S., Chivenge, P., Amouzou, K.A., Oberthur, T., Chakraborty, S., Sileshi, G.W., 2022. Novel insights into factors associated with yield response and nutrient use efficiency of maize and rice in sub-Saharan Africa. A review. Agron. Sustain. Dev. 42 (5). https://doi.org/10.1007/s13593-022-00821-4.

Zingore, S., Delve, R.J., Nyamangara, J., Giller, K.E., 2007. Multiple benefits of manure: the key to maintenance of soil fertility and restoration of depleted sandy soils on African smallholder farms. Nutr. Cycl. Agroecosystems 80 (3), 267–282. https://doi.org/10.1007/s10705-007-9142-2.